SAND2016-5893C

# Impact of Multiscale Characteristics of Heterogeneous Pore Structure and Mineralogy on Mechanical Properties of Shale

Hongkyu Yoon, Joseph Grigg, Thomas Dewers, Peter Mozley, Alex Rinehart, Jason Heath, Mathew Ingram

NEW MEXICO TECH
EARTH AND ENVIRONMENTAL SCIENCE

Sandia National Laboratories

# Introduction

- Predicting optimum zones for completion in shale difficult.
- Approach is to relate lithologic observations to mechanical properties at multiple scales.
- Use as data for mechanical modeling.

# Use of lithofacies in upscaling

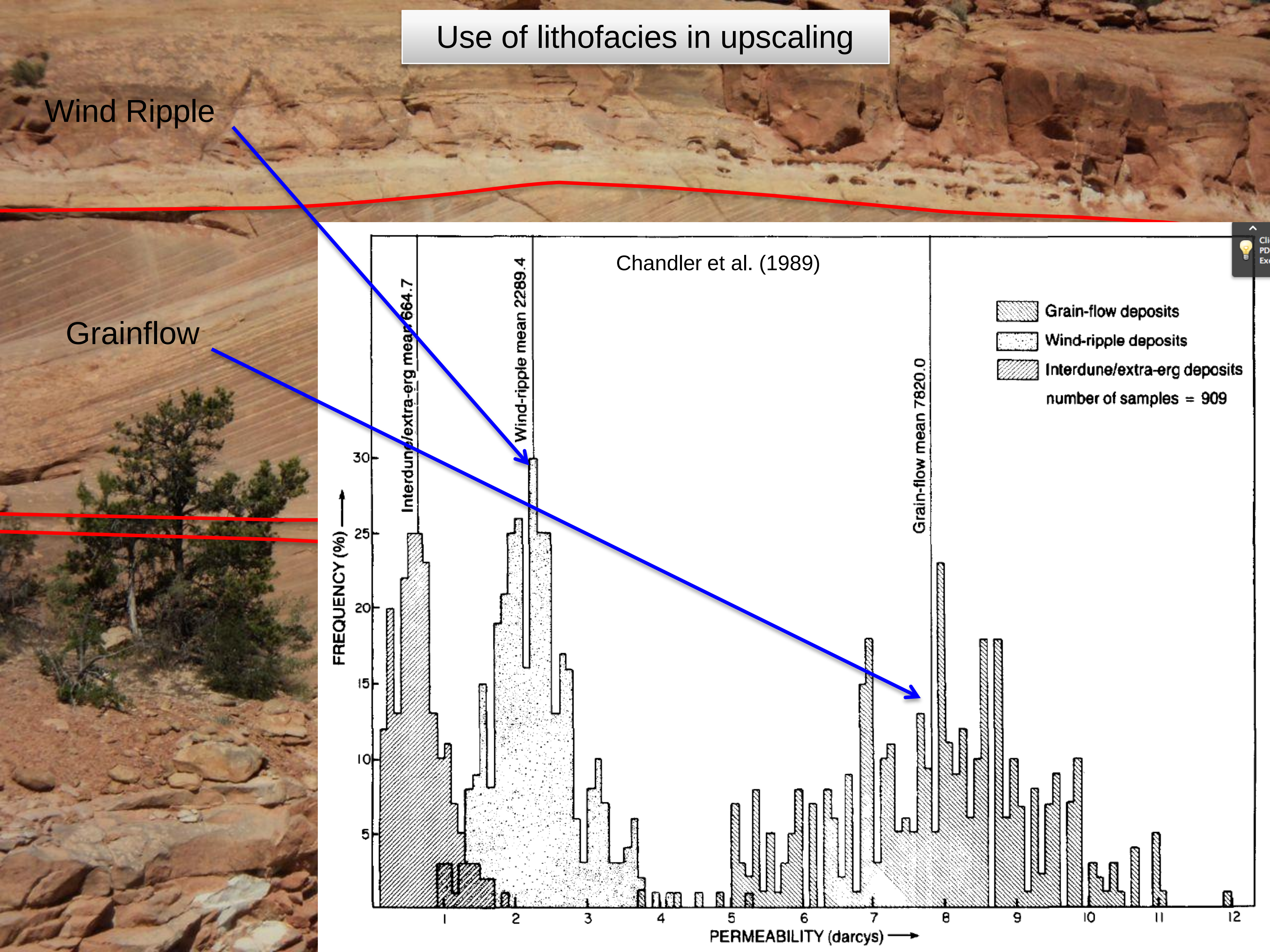

# Methods

- 40 cm diameter core from TerraTek quarry
- Mineralogical and textural characterization
  - Macroscopic
  - Optical petrography
  - BSE, X-ray mapping
  - Micro-CT
- Mechanical tests
  - Axisymmetric compression (1x2”)
  - Cylinder splitting (1x0.5”)
  - Mechanical modeling

# Mancos Shale

- Dark gray to black calcareous and noncalcareous shale
- Offshore and open-shallow marine environments
- Late Cretaceous Interior Seaway

- The "Cheese Wheel"
  - Interlaminated fine mud, medium/coarse mud, and very fine sand
  - 1-3 mm laminae
  - Parallel lamina, wavy-lenticular lamina, ripple forms, and bioturbation
  - Sandy medium Mudstone (smM)

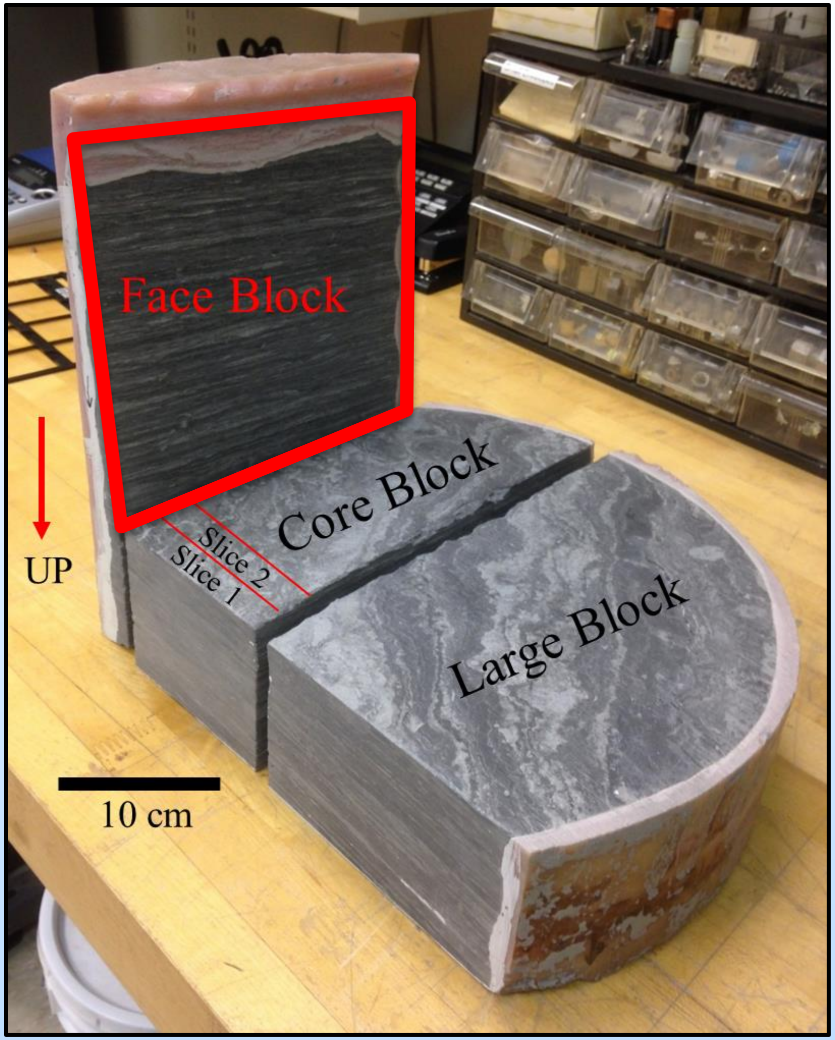


The Cheese Wheel


20 cm

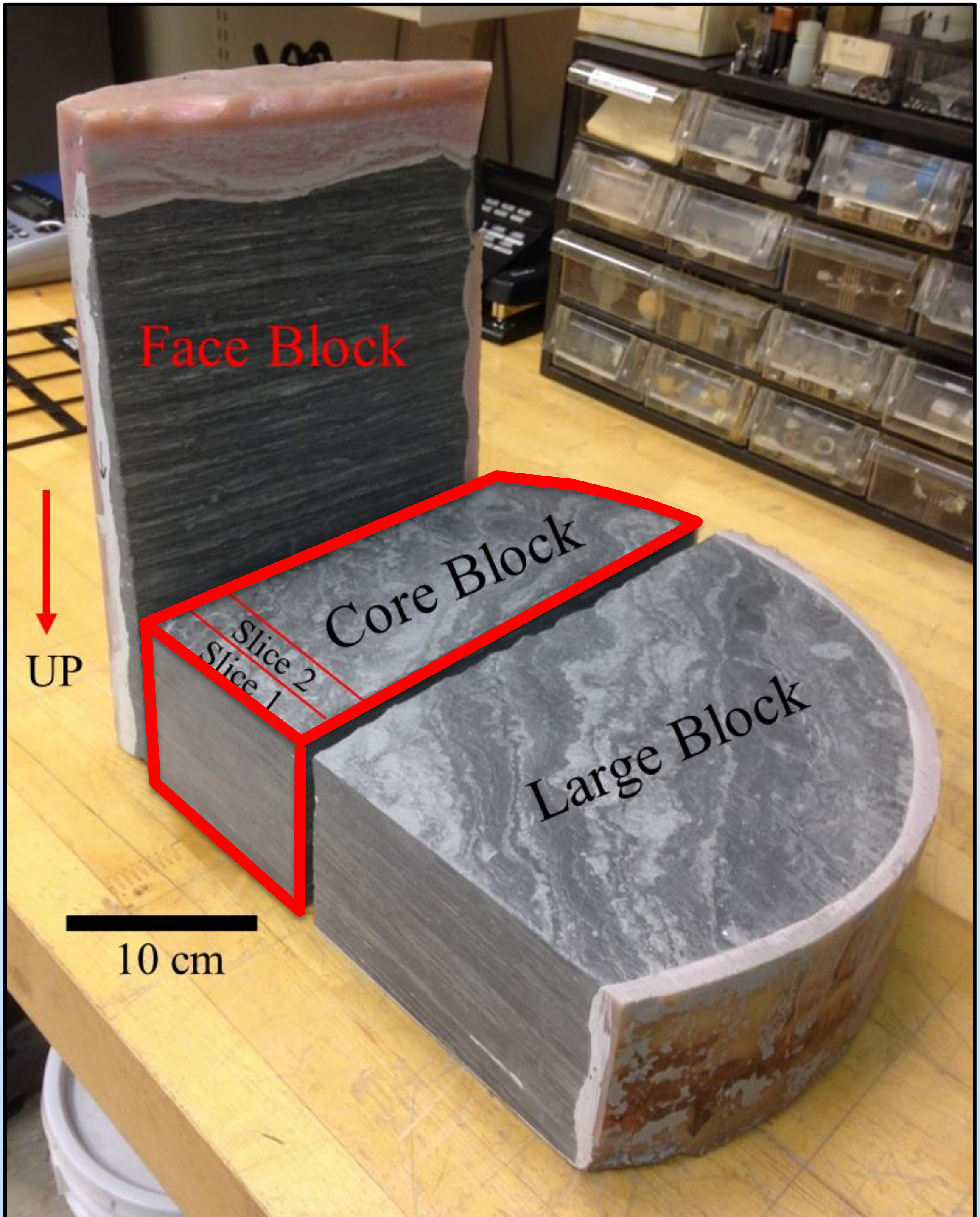
Face Block
Core Block
Slice 2
Slice 1
Large Block
UP
10 cm

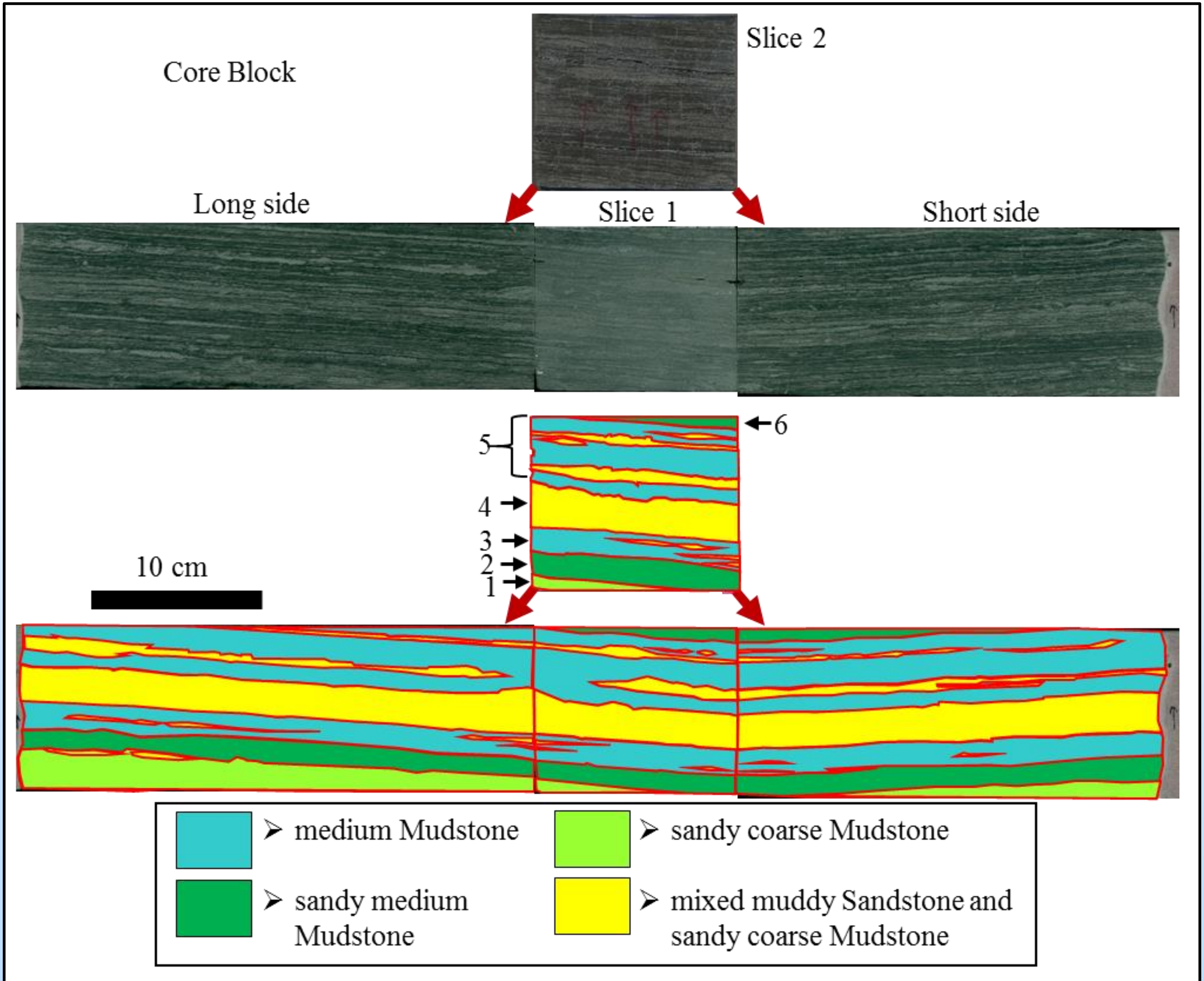
Core Block
Slice 2
Long side
Slice 1
Short side
5
6
4
3
2
1
10 cm
medium Mudstone
sandy coarse Mudstone
sandy medium Mudstone
mixed muddy Sandstone and sandy coarse Mudstone

# Macroscopic Description-XRD

- XRD is commonly used for baseline characterization

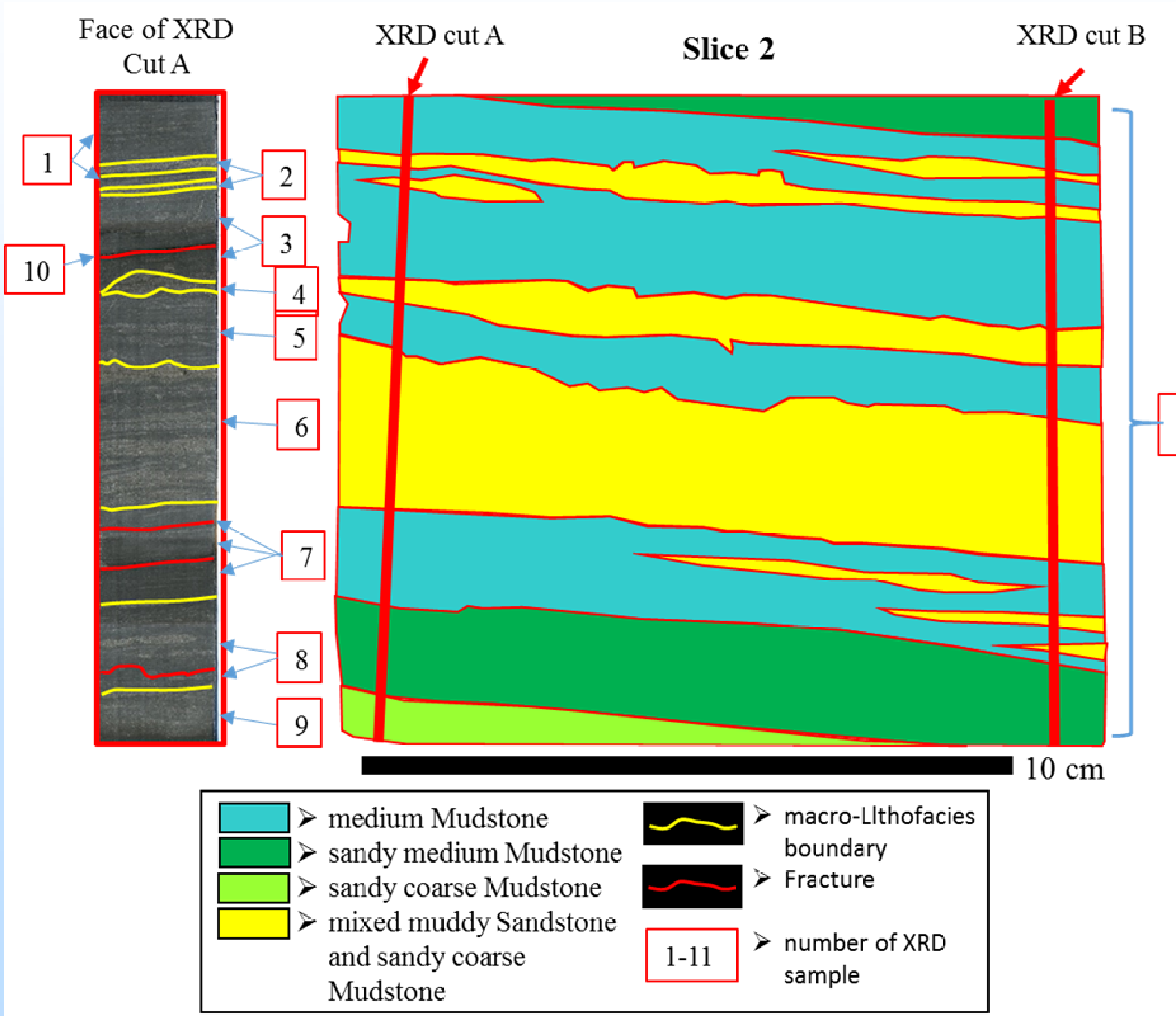

| Shale Formation | Proportion (%) | | |
|---|---|---|---|
| | Clay | Silica | CO3 |
| Eagle Ford Lo. | 18.9 | 20.5 | 60.6 |
| Eagle Ford Up. | 7.9 | 21.2 | 70.9 |
| Niobrara Chalk | 7.5 | 5 | 87.5 |
| Barnett | 29.6 | 53 | 17.4 |
| Bakken Silt | 10 | 20 | 70 |
| Bakken Shale | 31.2 | 43.8 | 25 |
| Fayettville | 30 | 40 | 30 |
| Haynesville | 33.7 | 35 | 31.3 |
| Pearsall | 15.3 | 31.8 | 52.9 |
| Three Forks | 31.0 | 28.0 | 41.0 |
| Sanish | 11.0 | 71.0 | 18.0 |
| Woodford | 8.0 | 70.0 | 22.0 |
| Marcellus | 50.0 | 30.0 | 20.0 |
| Pronghorn | 52.0 | 37.0 | 11.0 |
| Niobrara Marl | 13.0 | 22.0 | 65.0 |

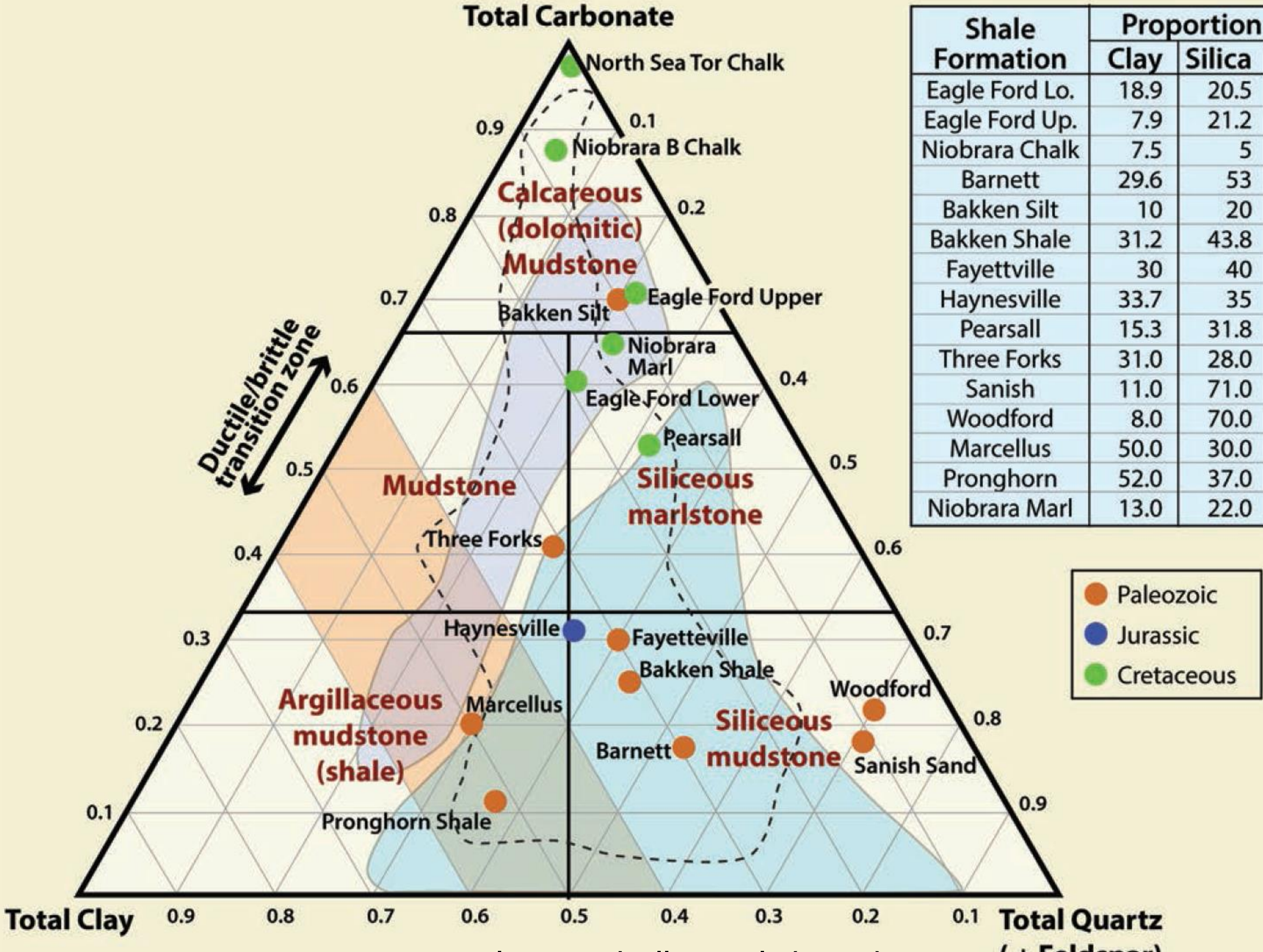


From: Ulmer-Scholle et al. (2014)

From: Hart et al. (2013)

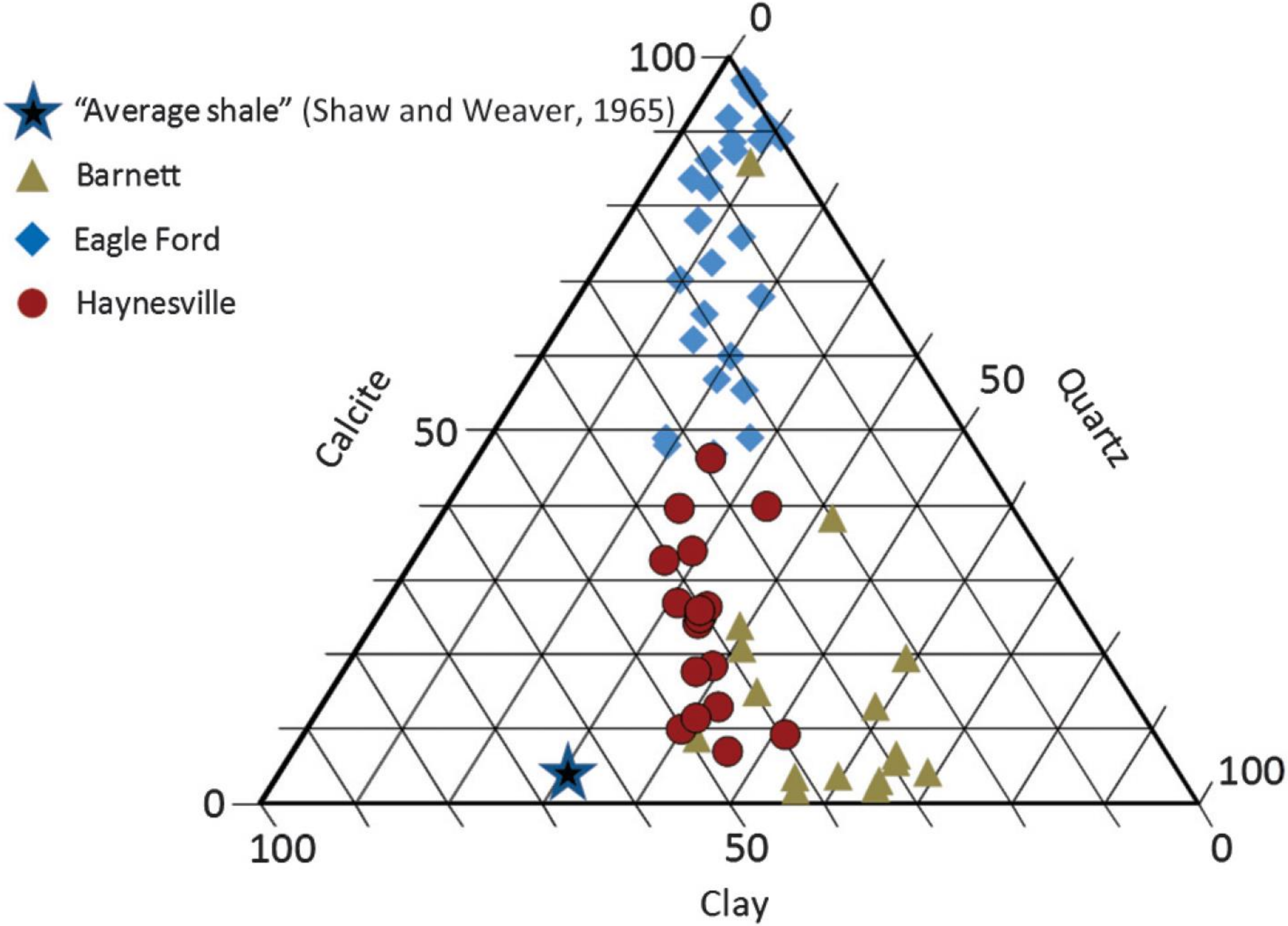

# Macroscopic Description-XRD

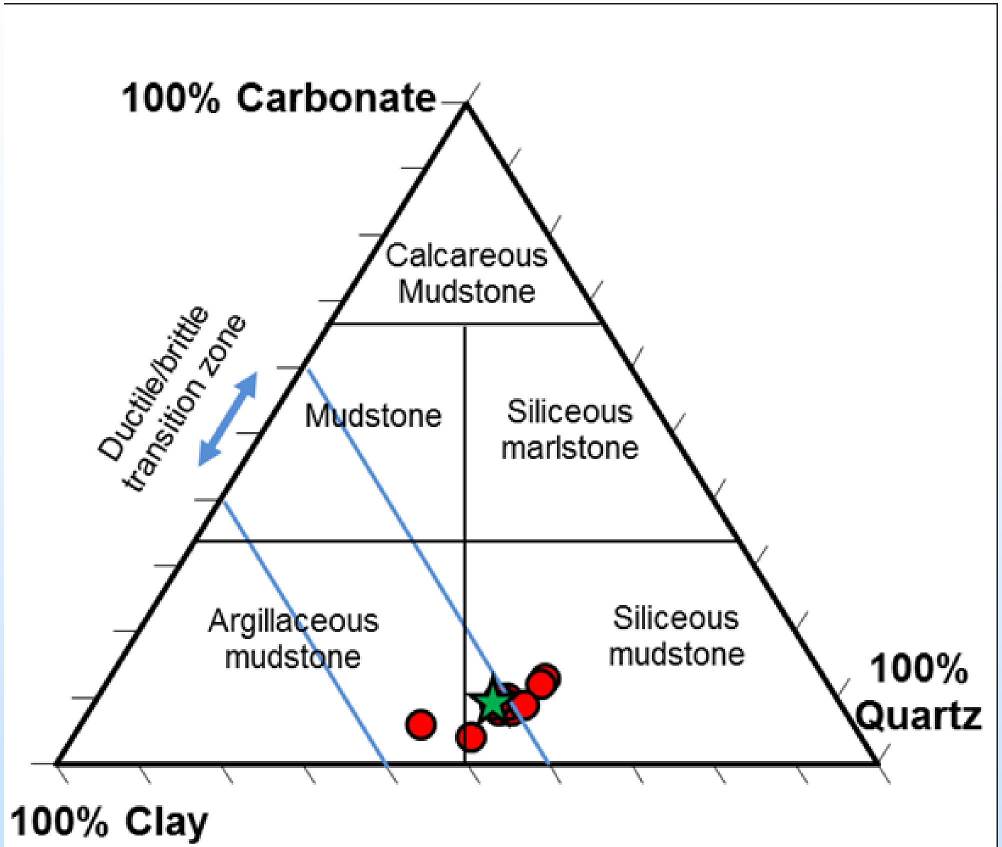


Mancos XRD Data

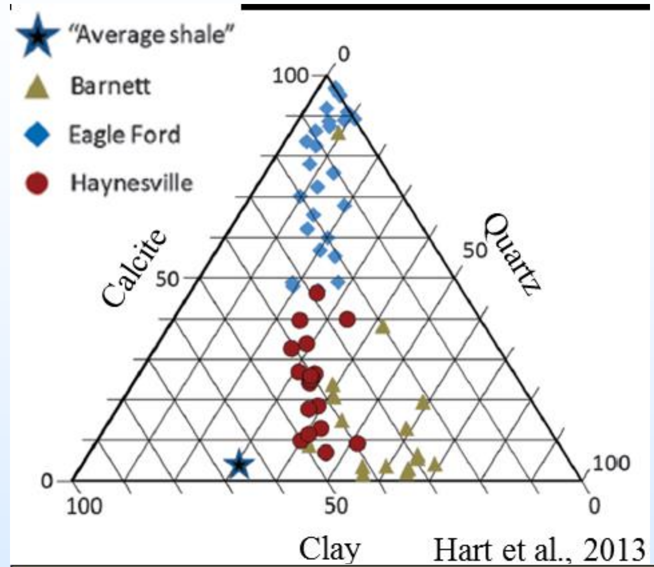


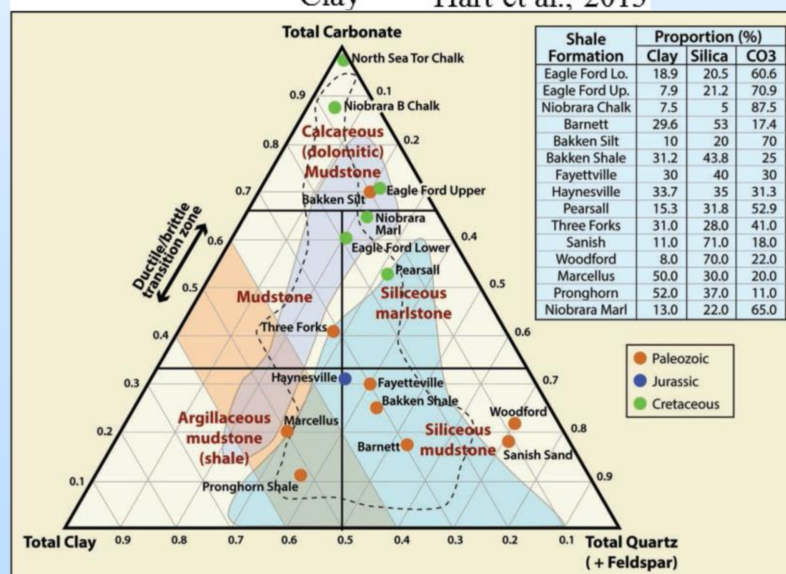


| Shale Formation | Proportion (%) | | |
|---|---|---|---|
| | Clay | Silica | CO3 |
| Eagle Ford Lo. | 18.9 | 20.5 | 60.6 |
| Eagle Ford Up. | 7.9 | 21.2 | 70.9 |
| Niobrara Chalk | 7.5 | 5 | 87.5 |
| Barnett | 29.6 | 53 | 17.4 |
| Bakken Silt | 10 | 20 | 70 |
| Bakken Shale | 31.2 | 43.8 | 25 |
| Fayettville | 30 | 40 | 30 |
| Haynesville | 33.7 | 35 | 31.3 |
| Pearsall | 15.3 | 31.8 | 52.9 |
| Three Forks | 31.0 | 28.0 | 41.0 |
| Sanish | 11.0 | 71.0 | 18.0 |
| Woodford | 8.0 | 70.0 | 22.0 |
| Marcellus | 50.0 | 30.0 | 20.0 |
| Pronghorn | 52.0 | 37.0 | 11.0 |
| Niobrara Marl | 13.0 | 22.0 | 65.0 |

- Macro-lithofacies consist of several micro-lithofacies

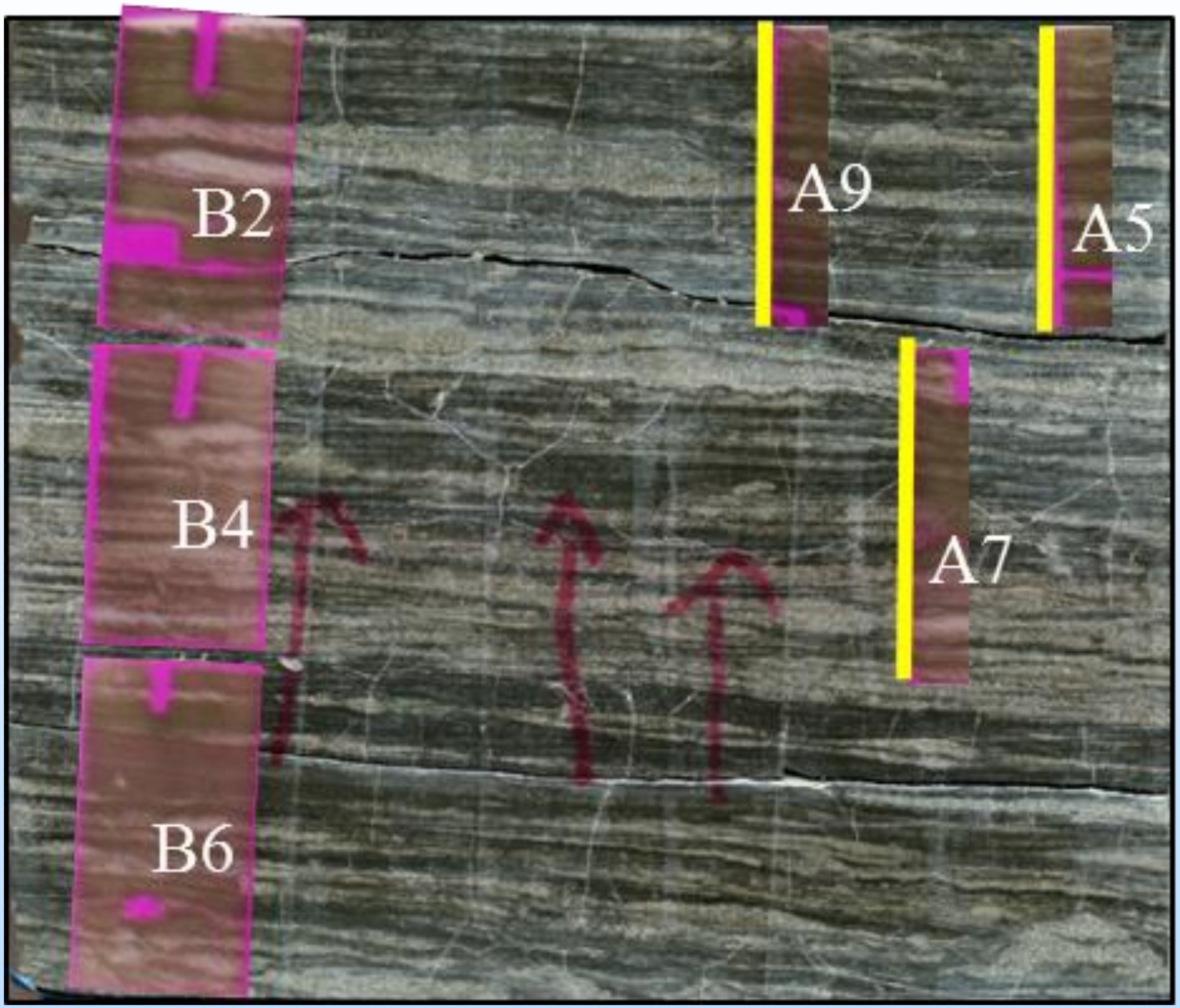

# Microscopic Description-Petrography

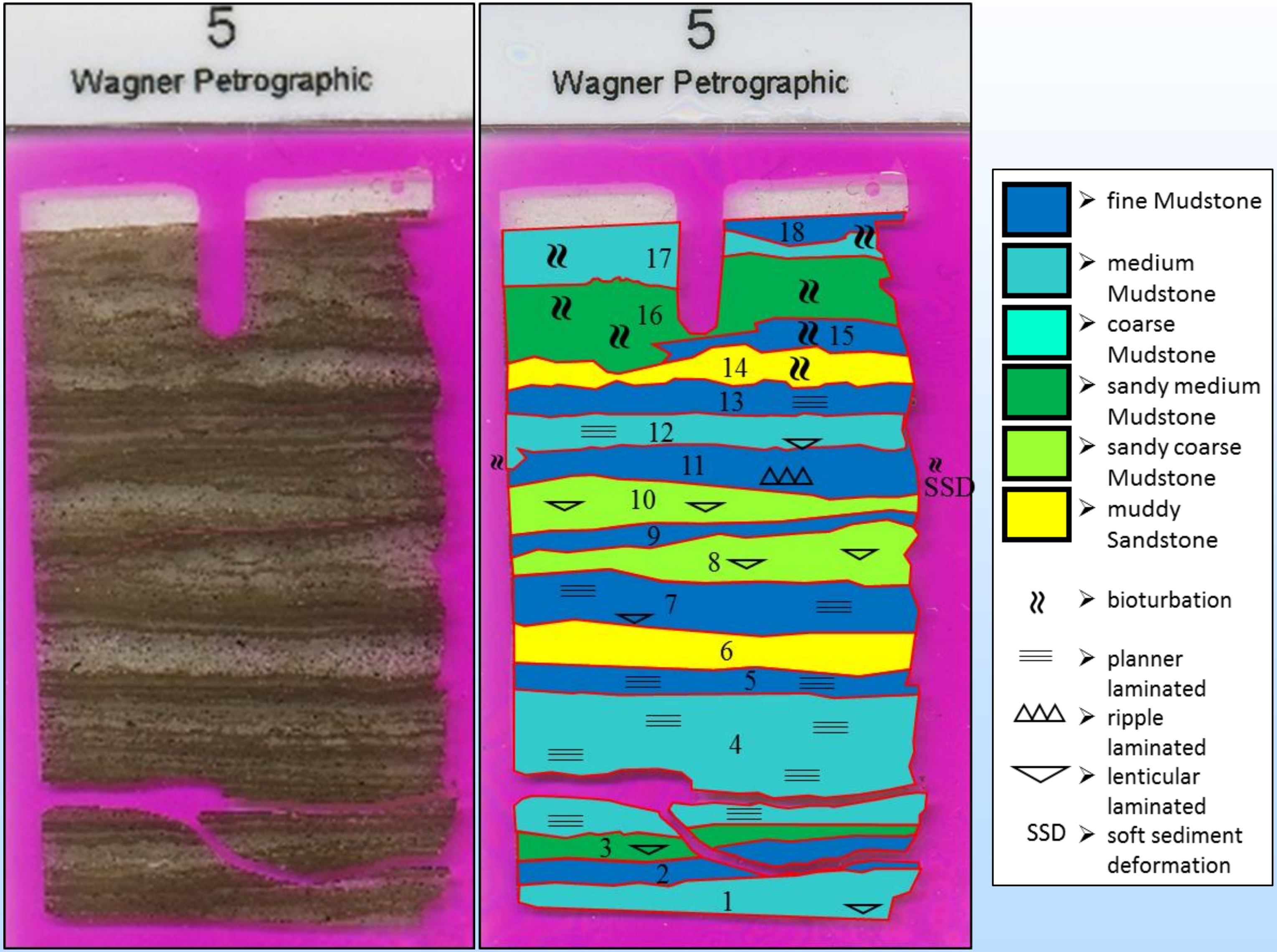

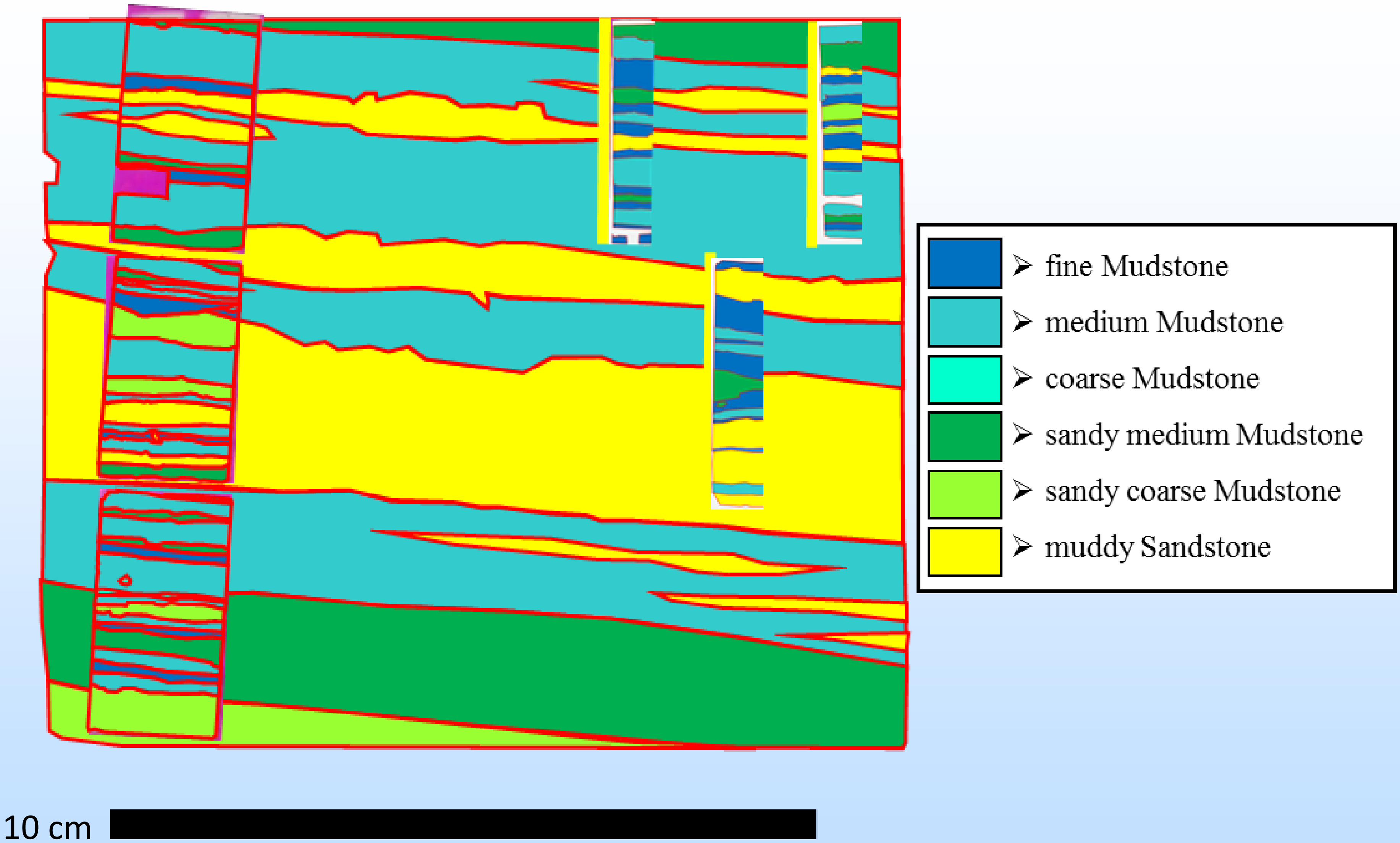
fine Mudstone
medium Mudstone
coarse Mudstone
sandy medium Mudstone
sandy coarse Mudstone
muddy Sandstone
10 cm

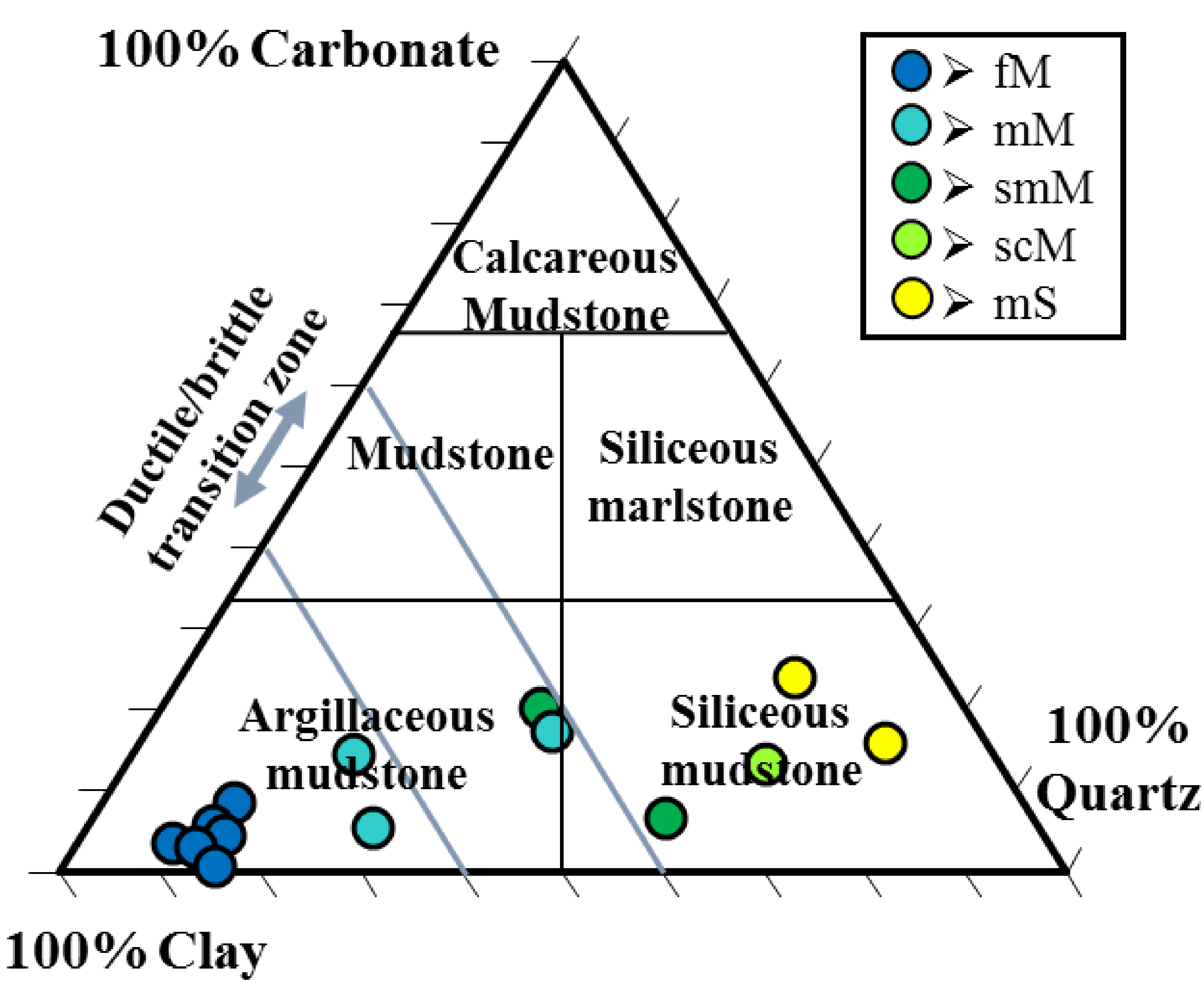
100% Carbonate
Calcareous Mudstone
Mudstone
Siliceous marlstone
Argillaceous mudstone
Siliceous mudstone
Ductile/brittle transition zone
100% Quartz
100% Clay
fM
mM
smM
scM
mS

# Compositional Heterogeneity

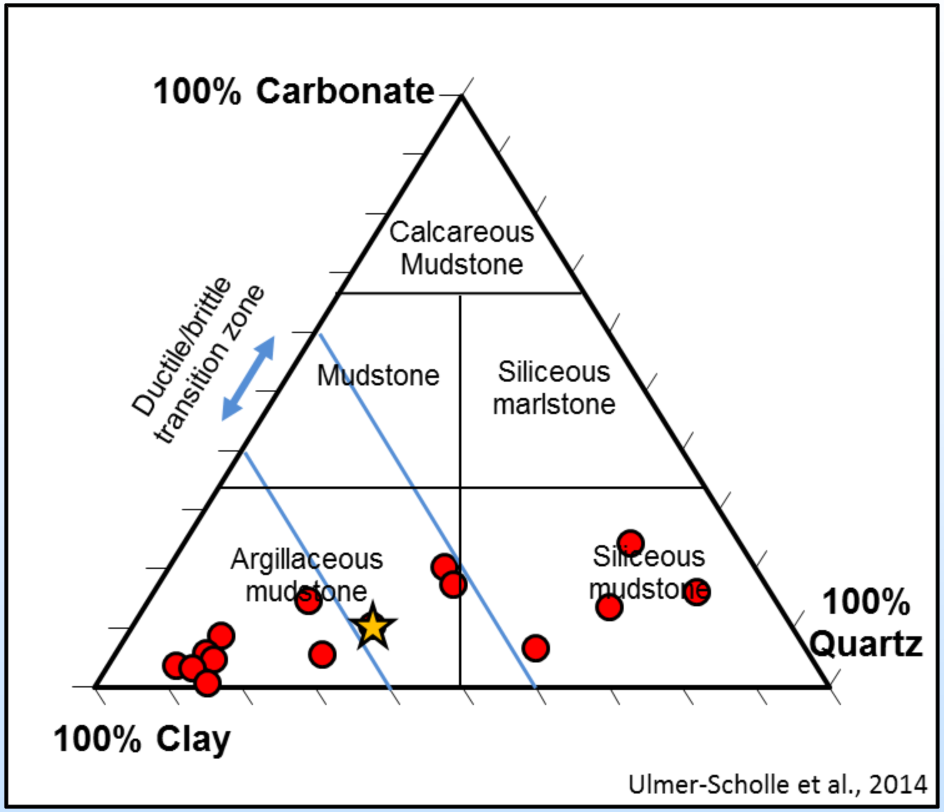


Microlithofacies composition (petrograpy)

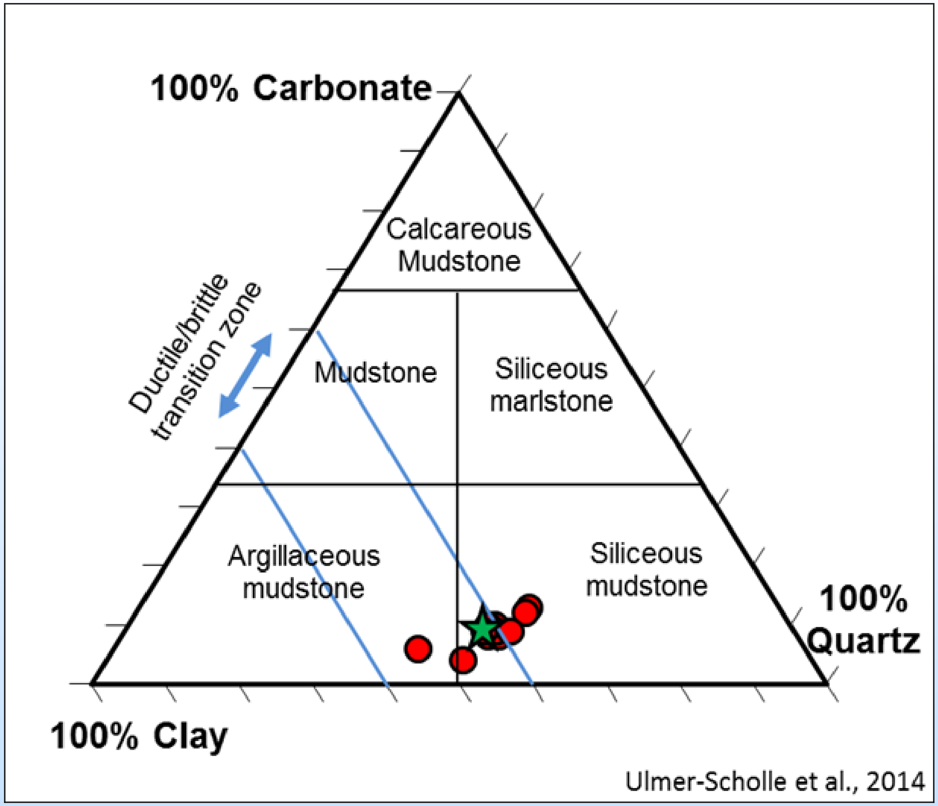


Macrolithofacies composition (XRD)

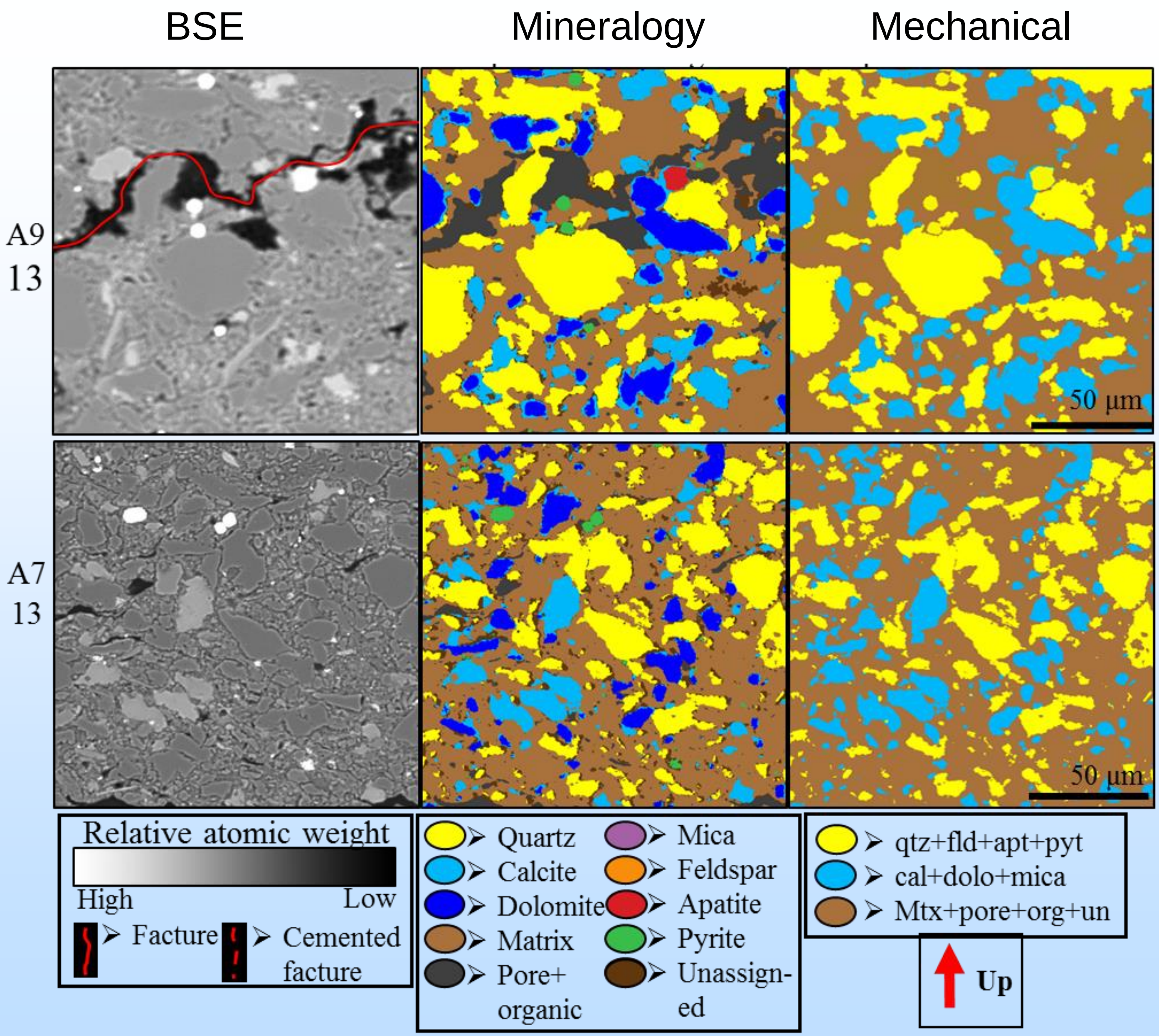
BSE
Mineralogy
Mechanical
A9
13
A7
13
50 μm
50 μm
Relative atomic weight
High
Low
Facture
Cemented facture
Quartz
Calcite
Dolomite
Matrix
Pore+ organic
Mica
Feldspar
Apatite
Pyrite
Unassign-ed
qtz+fld+apt+pyt
cal+dolo+mica
Mtx+pore+org+un
Up

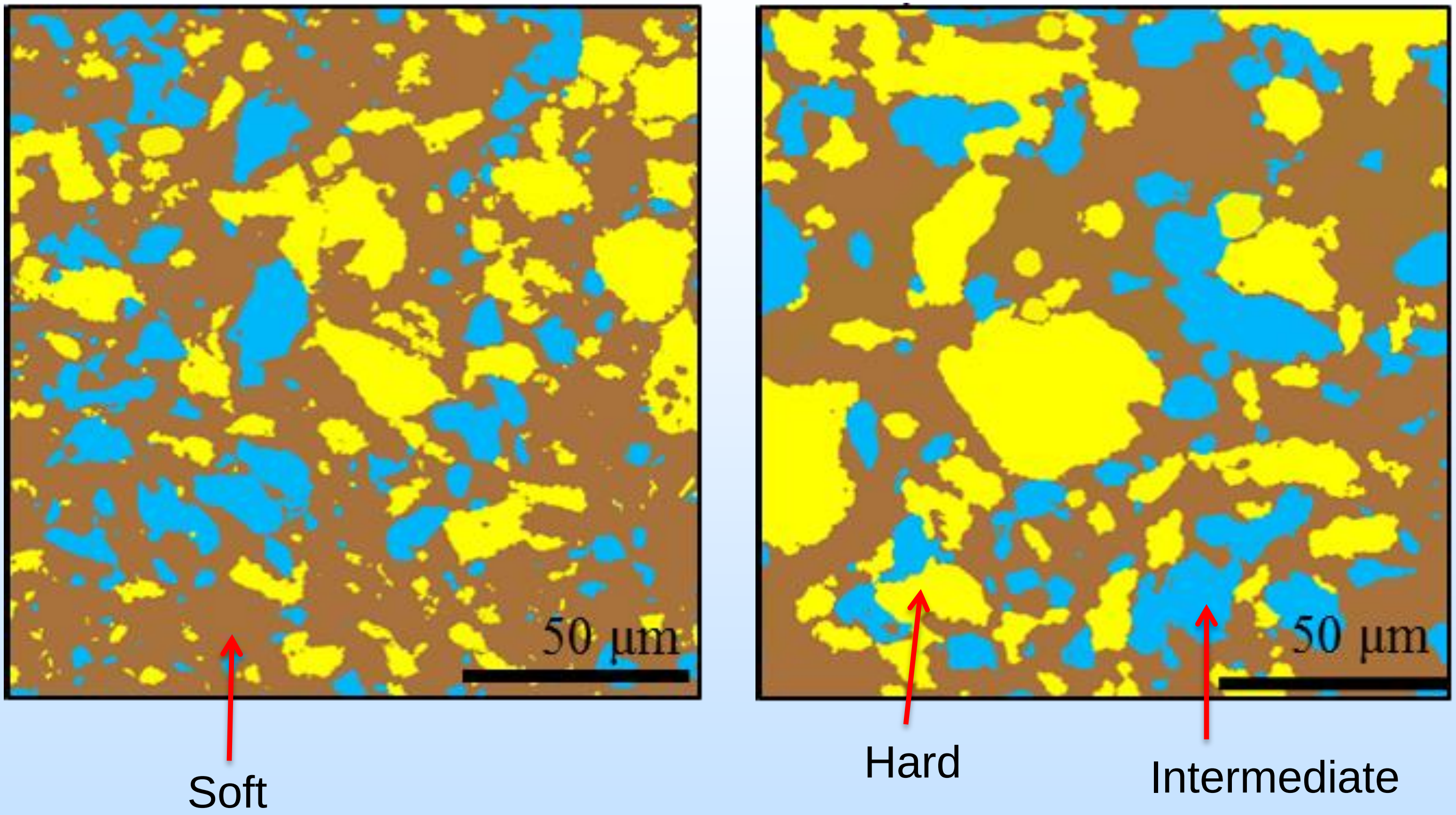
50 µm
50 µm
Soft
Hard
Intermediate

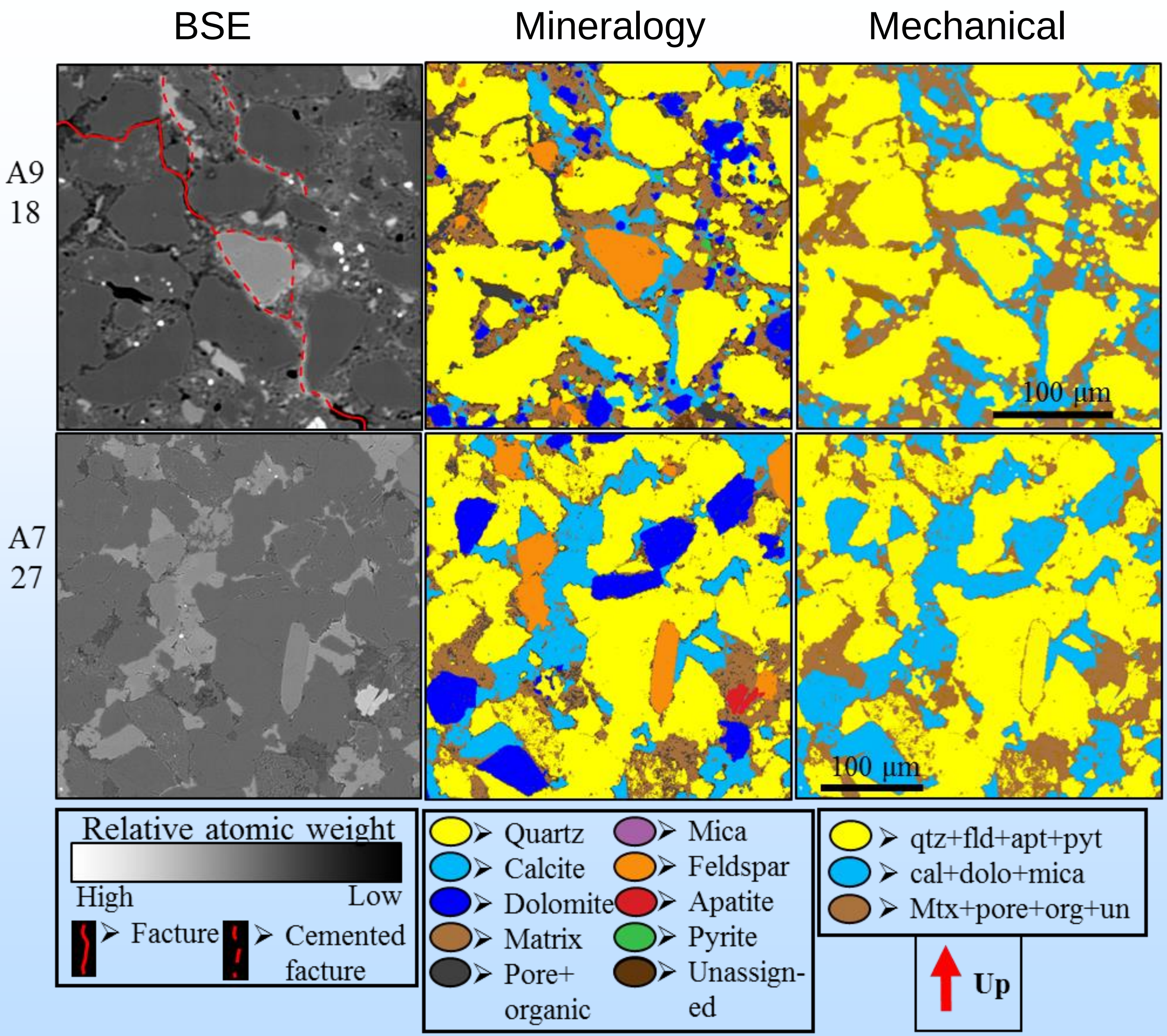

BSE
Mineralogy
Mechanical
A9
18
A7
27
100 µm
100 µm
Relative atomic weight
High
Low
Facture
Cemented
facture
Quartz
Calcite
Dolomite
Matrix
Pore+
organic
Mica
Feldspar
Apatite
Pyrite
Unassign-
ed
qtz+fld+apt+pyt
cal+dolo+mica
Mtx+pore+org+un
Up

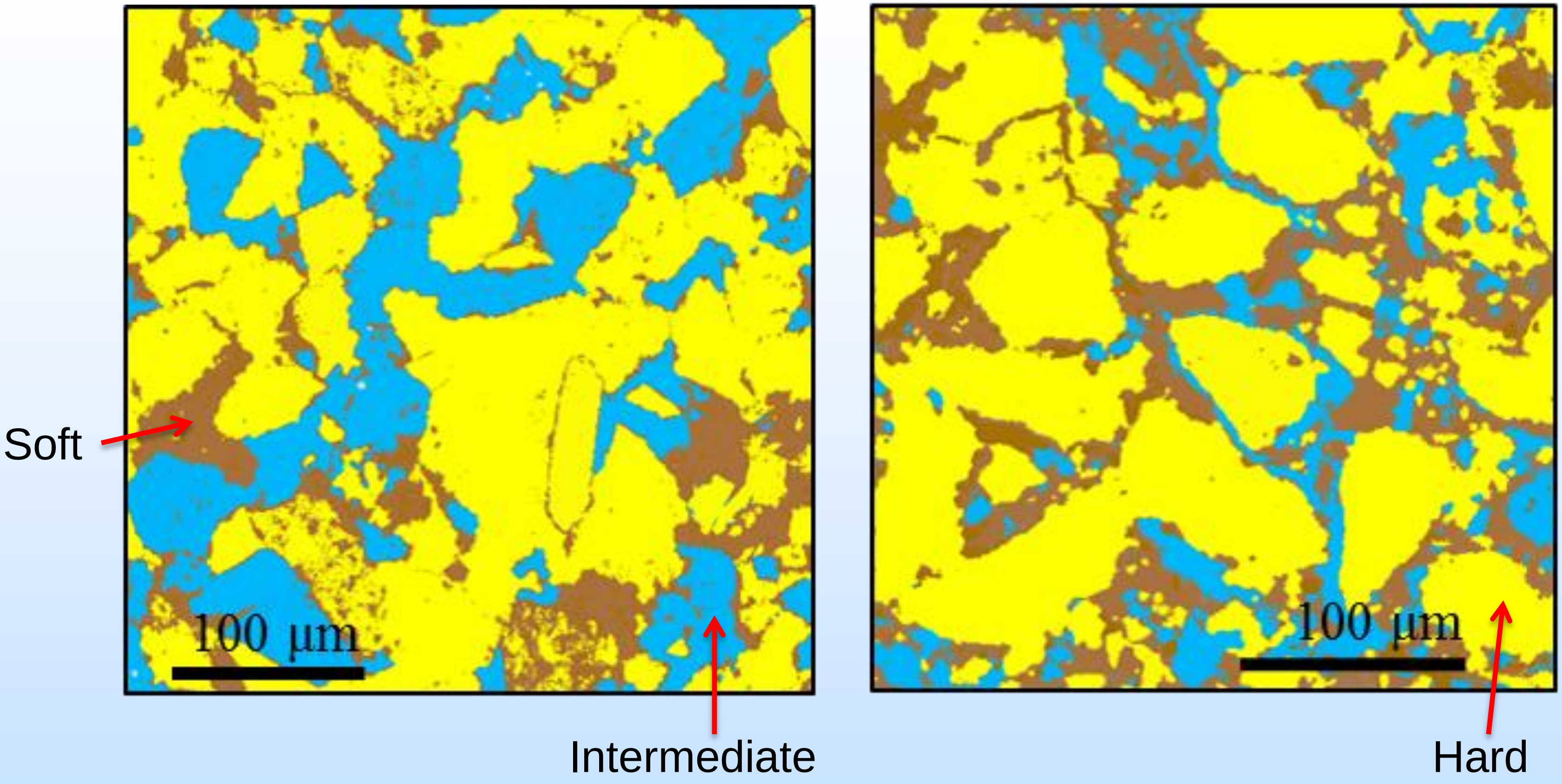
Soft
100 µm
Intermediate
100 µm
Hard

# Mechanical Testing

- High Bay Compressive Tests
  - Eight Tests
  - Two tests run at each condition
    - Unconfined (UCS)
    - 50 MPa Mean Stress
    - 100 MPa Mean Stress
    - 200 MPa Mean Stress
  - Perpendicular and parallel to bedding
  - Brazilian Tensile Strength Test
    - Four tests
      - One perpendicular to bedding
      - One at 45 degrees to bedding
      - Two parallel to bedding

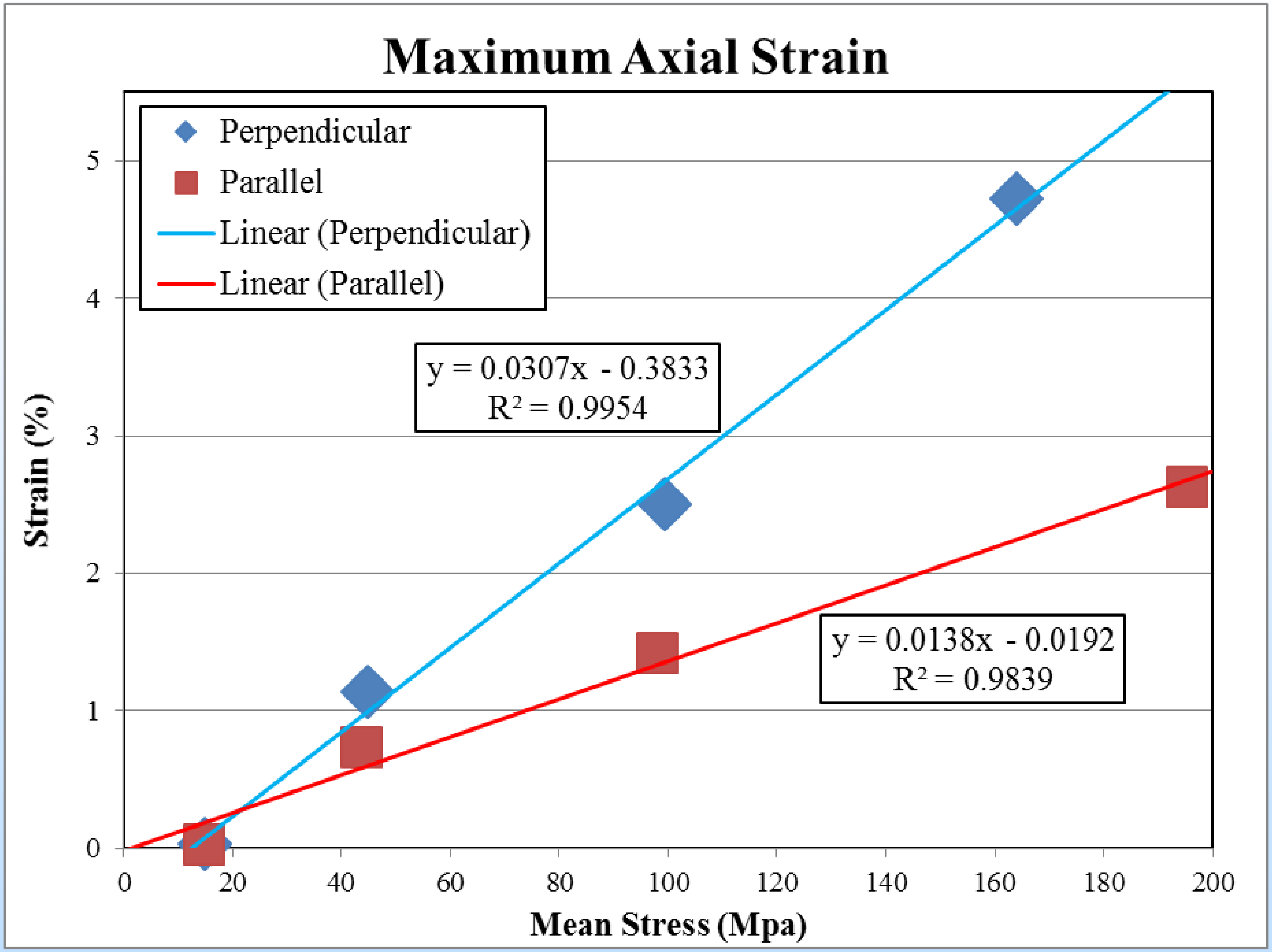

Maximum Axial Strain
Perpendicular
Parallel
Linear (Perpendicular)
Linear (Parallel)
y = 0.0307x - 0.3833
R² = 0.9954
y = 0.0138x - 0.0192
R² = 0.9839
Strain (%)
0
1
2
3
4
5
0
20
40
60
80
100
120
140
160
180
200
Mean Stress (Mpa)

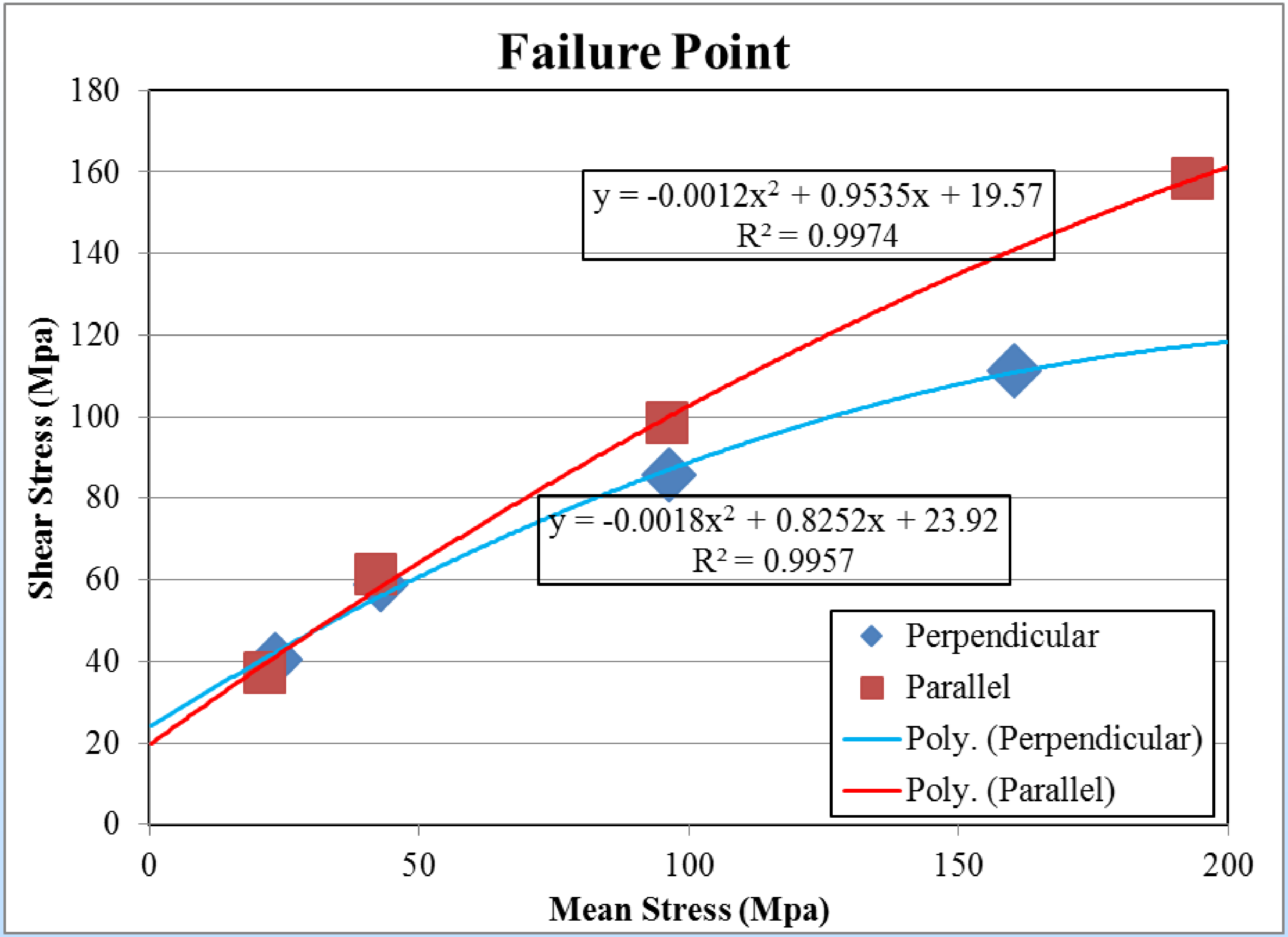
Failure Point
y = -0.0012x² + 0.9535x + 19.57
R² = 0.9974
y = -0.0018x² + 0.8252x + 23.92
R² = 0.9957
Perpendicular
Parallel
Poly. (Perpendicular)
Poly. (Parallel)
Shear Stress (Mpa)
Mean Stress (Mpa)
0
20
40
60
80
100
120
140
160
180
0
50
100
150
200

# Geomechanics-Conceptual Model

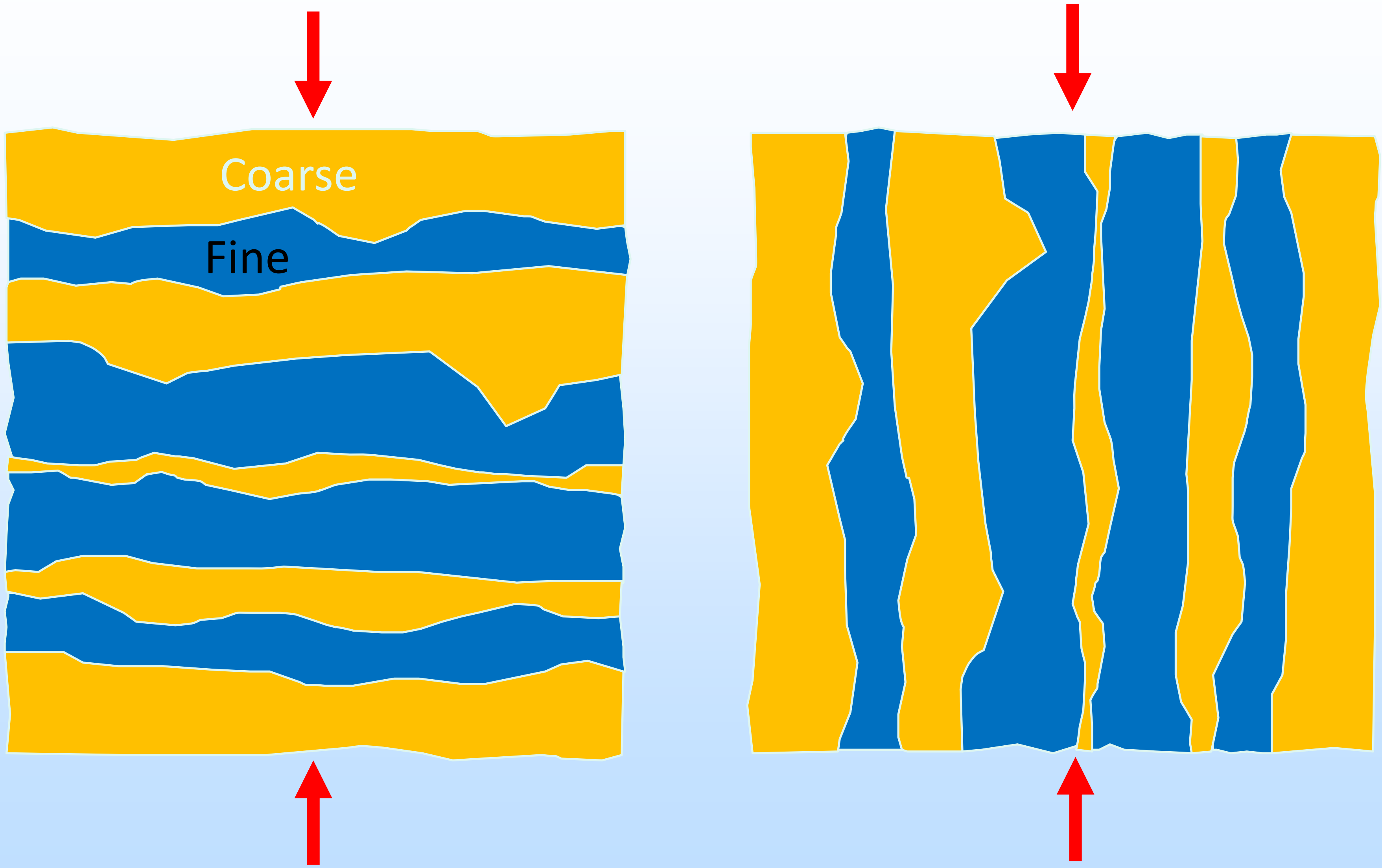

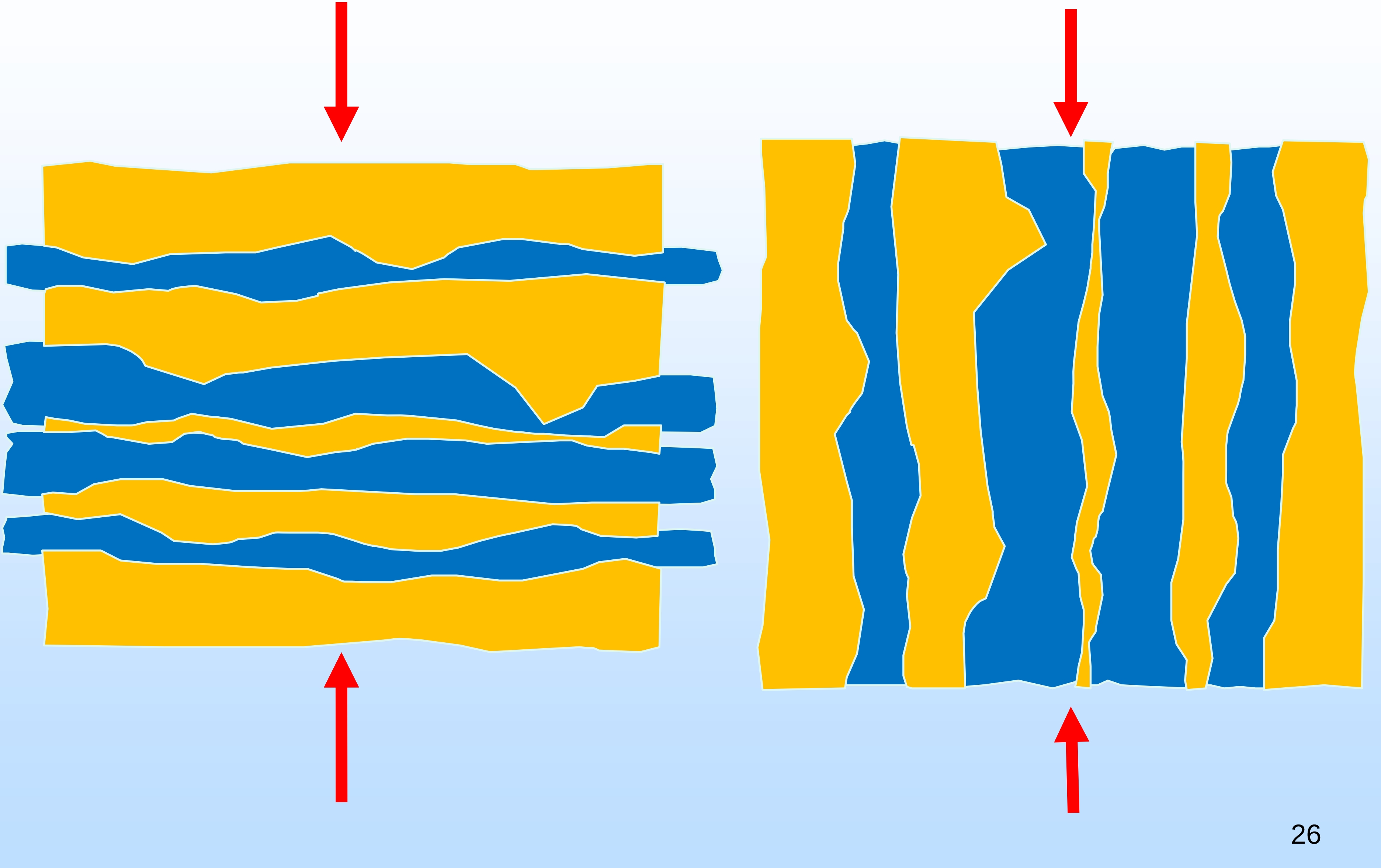

# Relating Heterogeneity to Strain

- Multiple scale micro-CT image stacks for Mancos shale

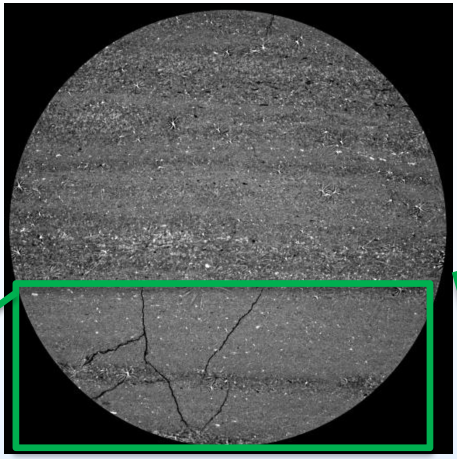

MicroCT Image of 1” core Mancos shale (17 microns resolution)

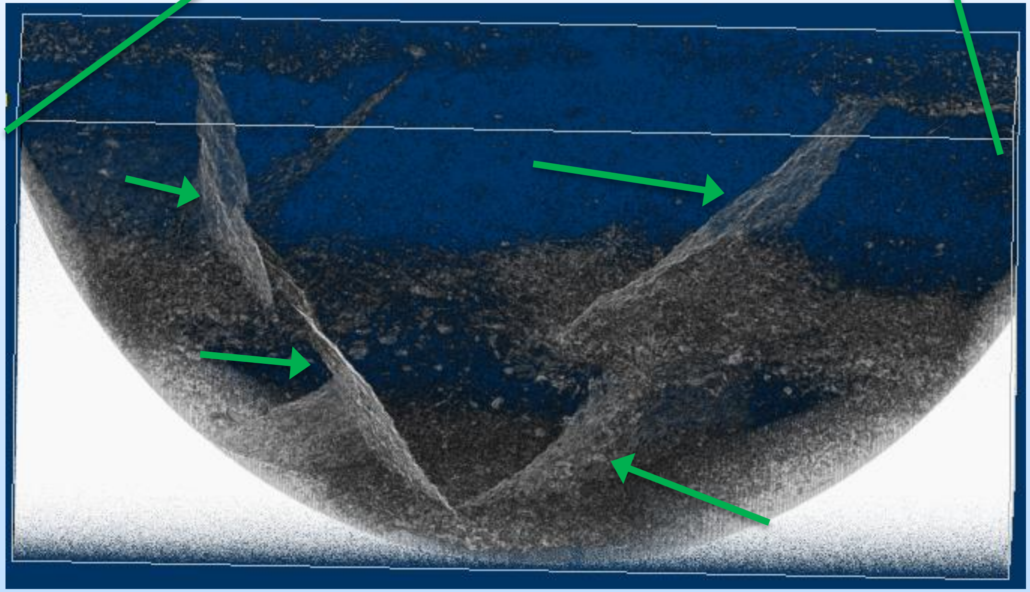

3D view of natural and artificial fractures (arrows) in clay-rich weak layers terminated by stiff layers. Relatively large white spots represent pyrites that are used to estimate 3D deformation of shale during mechanical testing


Estwing

Indirect Tensile (Brazilian Tests)

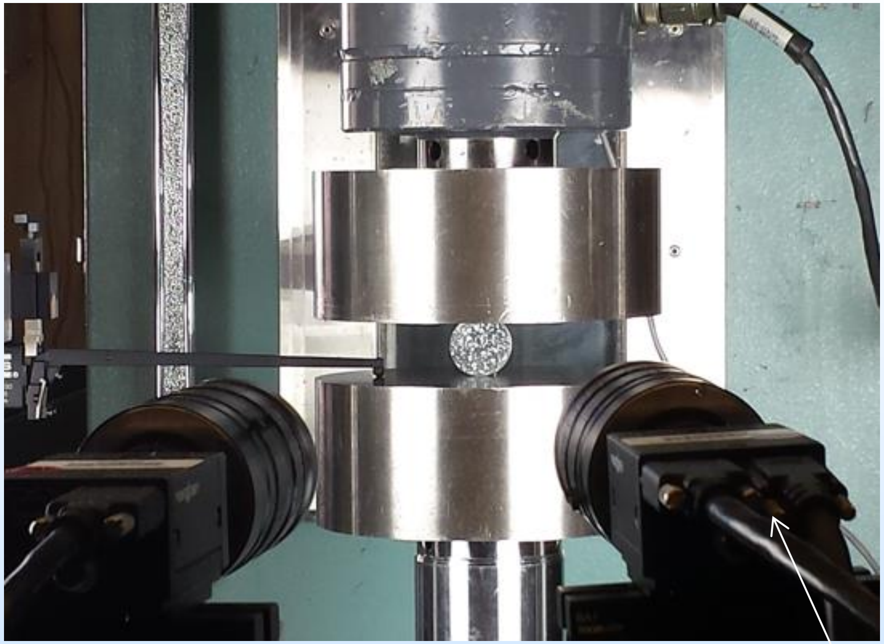

Indirect Tensile (Brazilian Test)

High speed camera

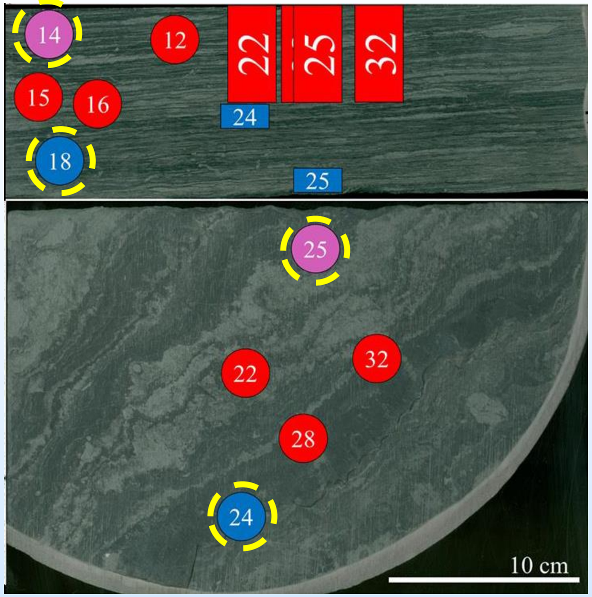


Two perpendicular and two parallel to bedding samples

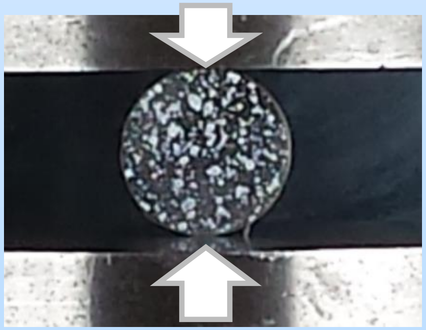

Paint markers: Digital Image Correlation to estimate 2D strain on the surface

# Indirect Tension Test Results

P: Loading

$$\sigma_t = \frac{2P}{\pi D t}$$

D: Diameter

t: thickness

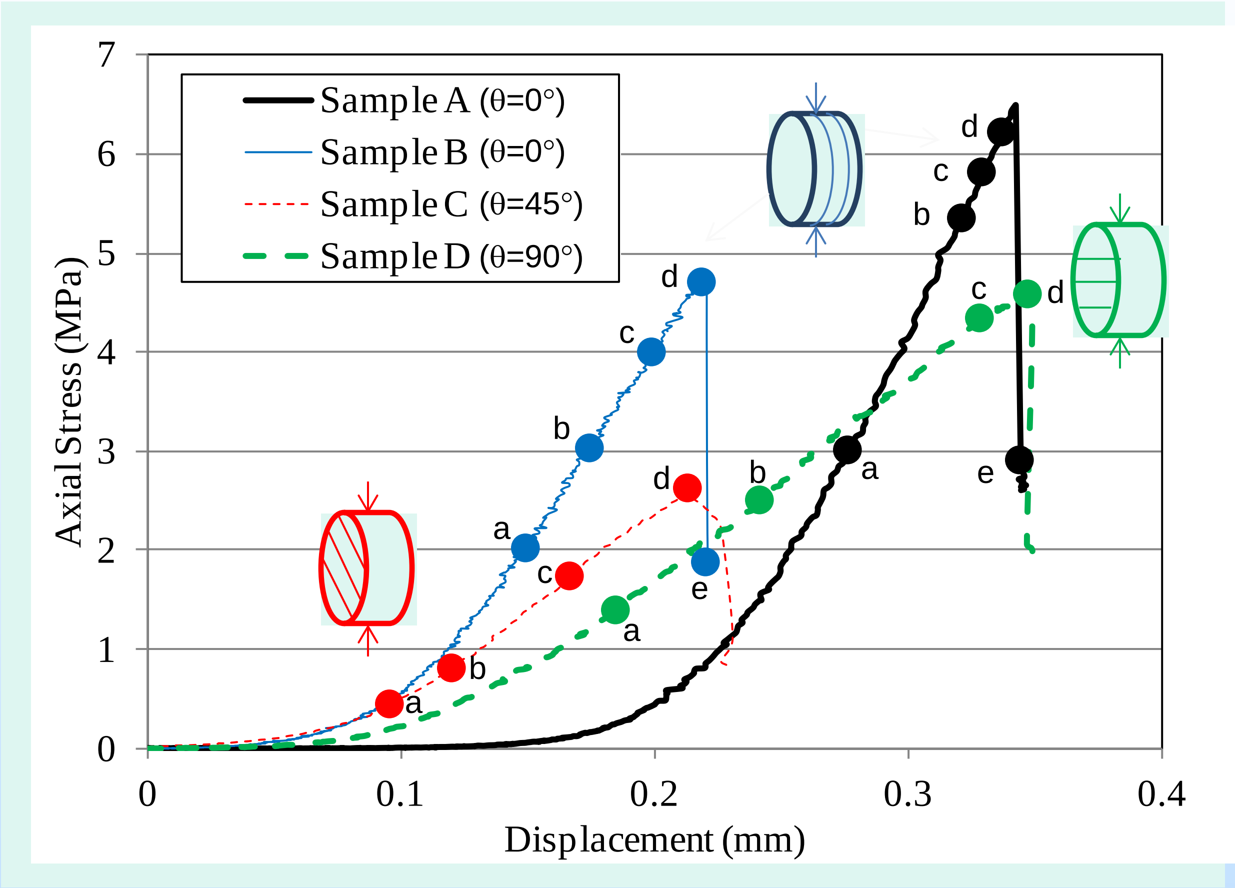

# Tensile Strain Distribution (Digital Image Correlation)

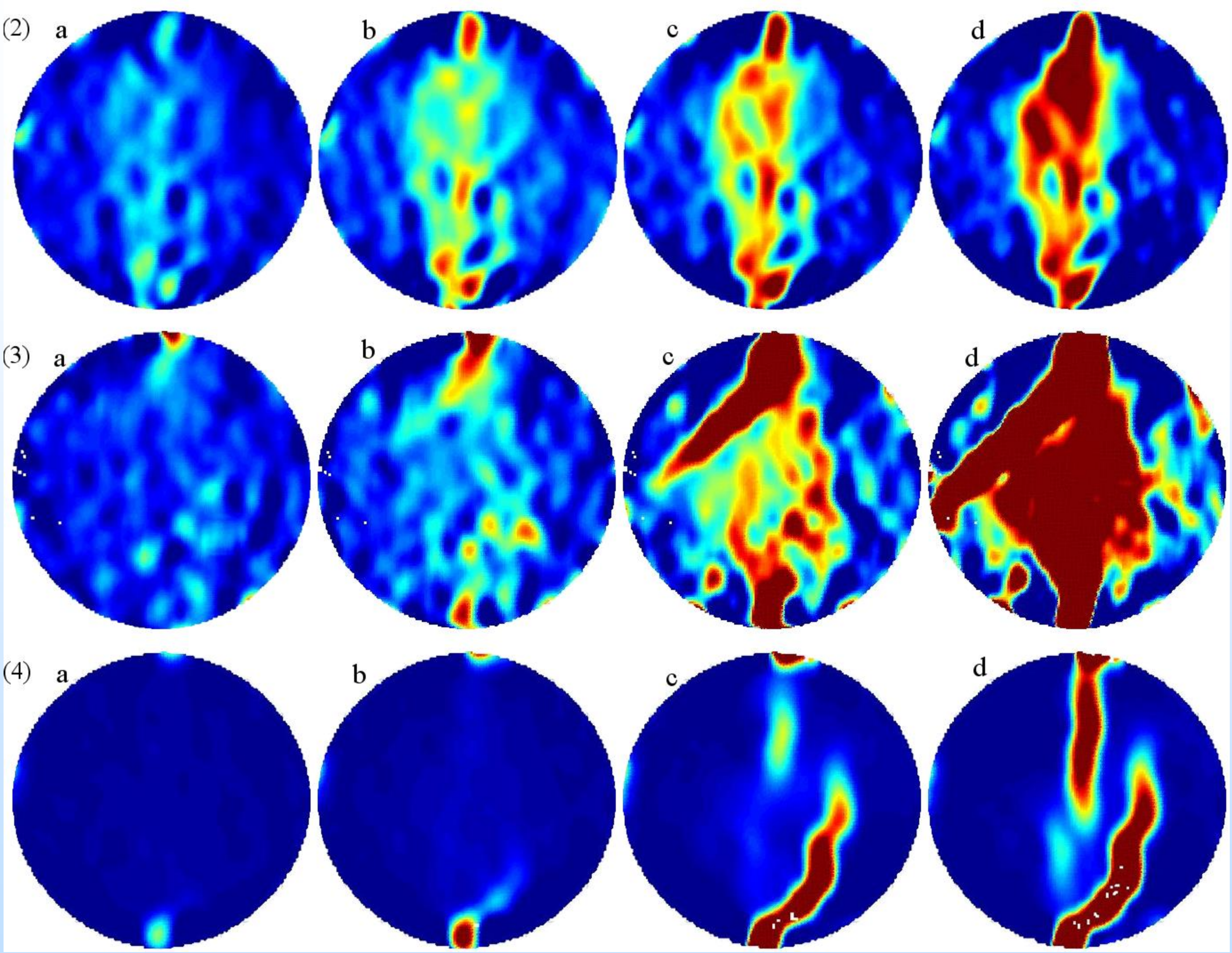


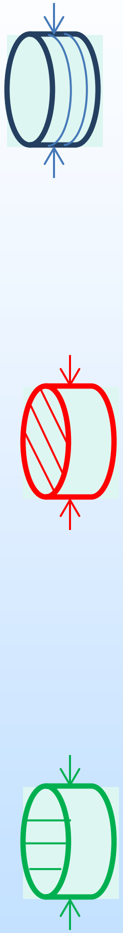

# Indirect Tension Test Results

Front

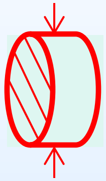

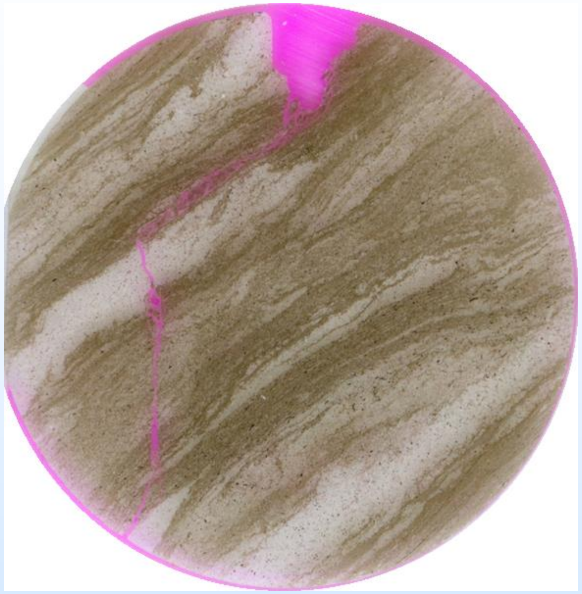

Back

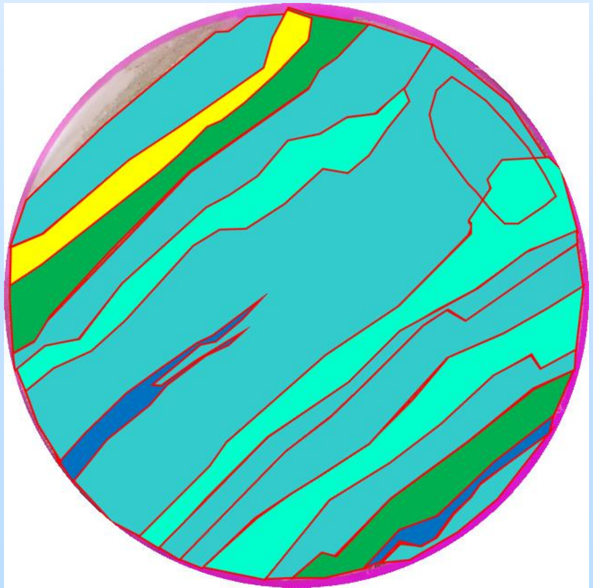

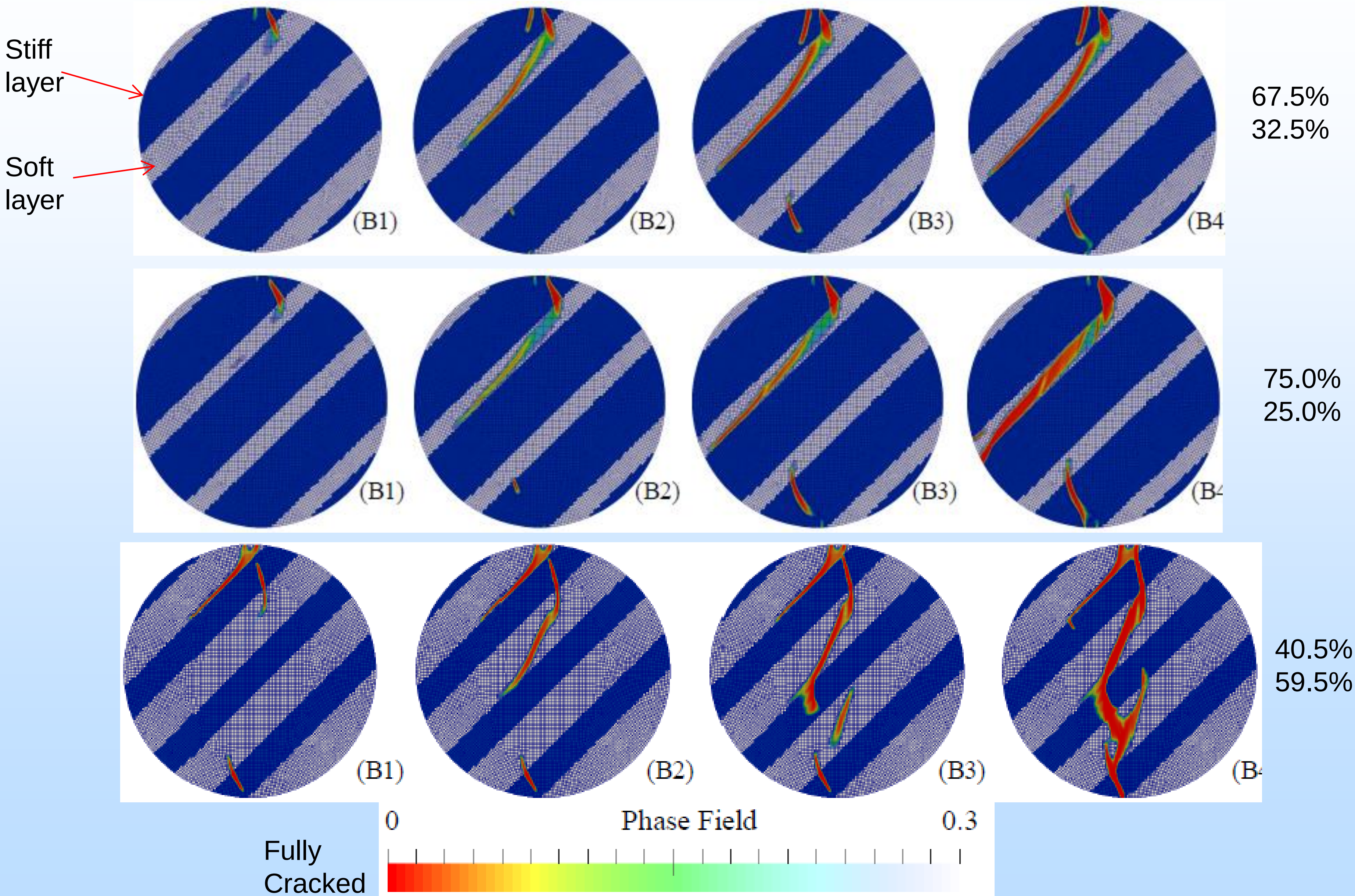
Stiff layer
Soft layer
(B1)
(B2)
(B3)
(B4
67.5%
32.5%
75.0%
25.0%
40.5%
59.5%
Fully Cracked
0
Phase Field
0.3


Outdoor

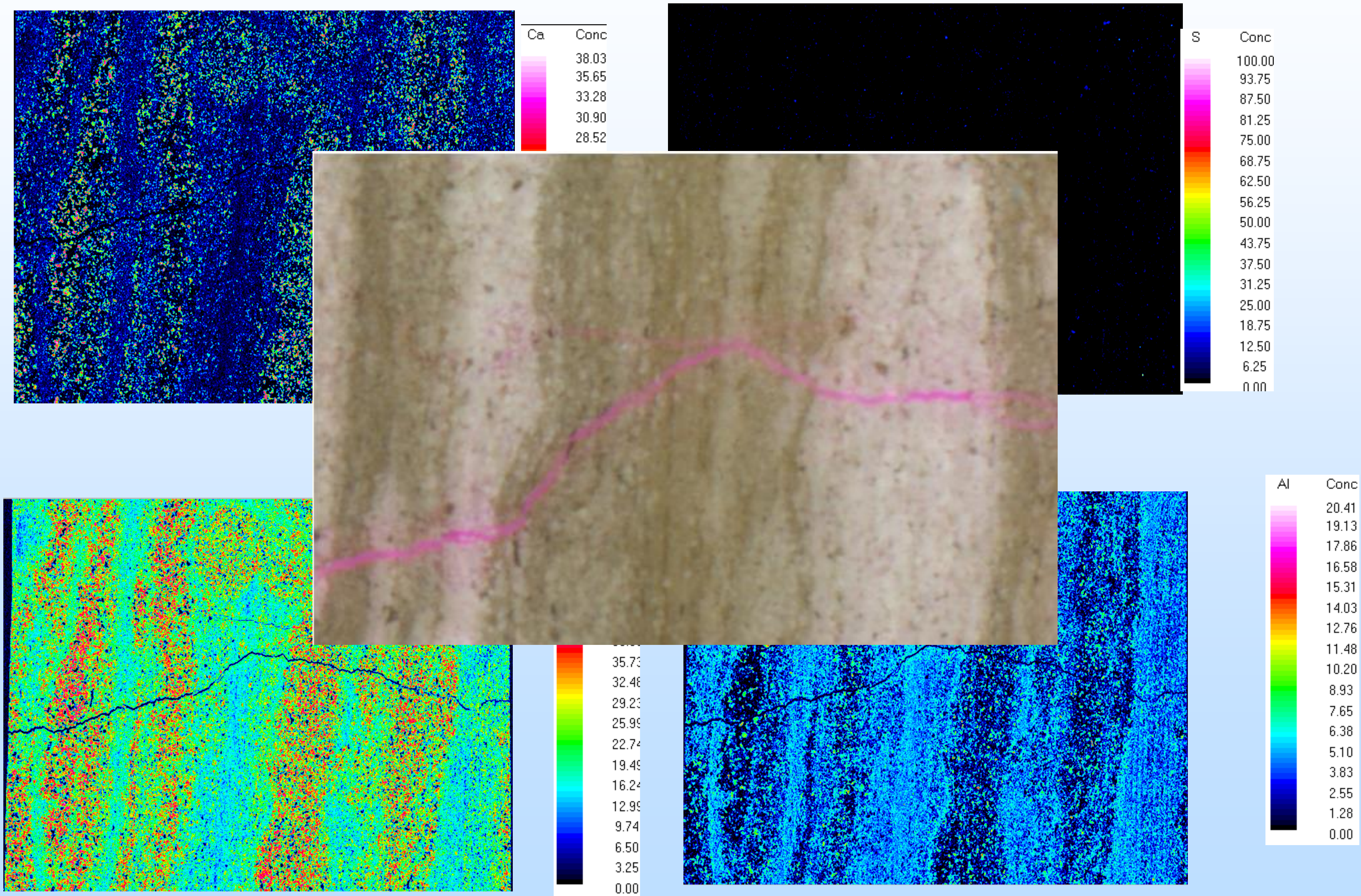

Ca
Conc
38.03
35.65
33.28
30.90
28.52
S
Conc
100.00
93.75
87.50
81.25
75.00
68.75
62.50
56.25
50.00
43.75
37.50
31.25
25.00
18.75
12.50
6.25
0.00
9.74
6.50
3.25
0.00
Al
Conc
20.41
19.13
17.86
16.58
15.31
14.03
12.76
11.48
10.20
8.93
7.65
6.38
5.10
3.83
2.55
1.28
0.00

# Micropillar Compression Testing

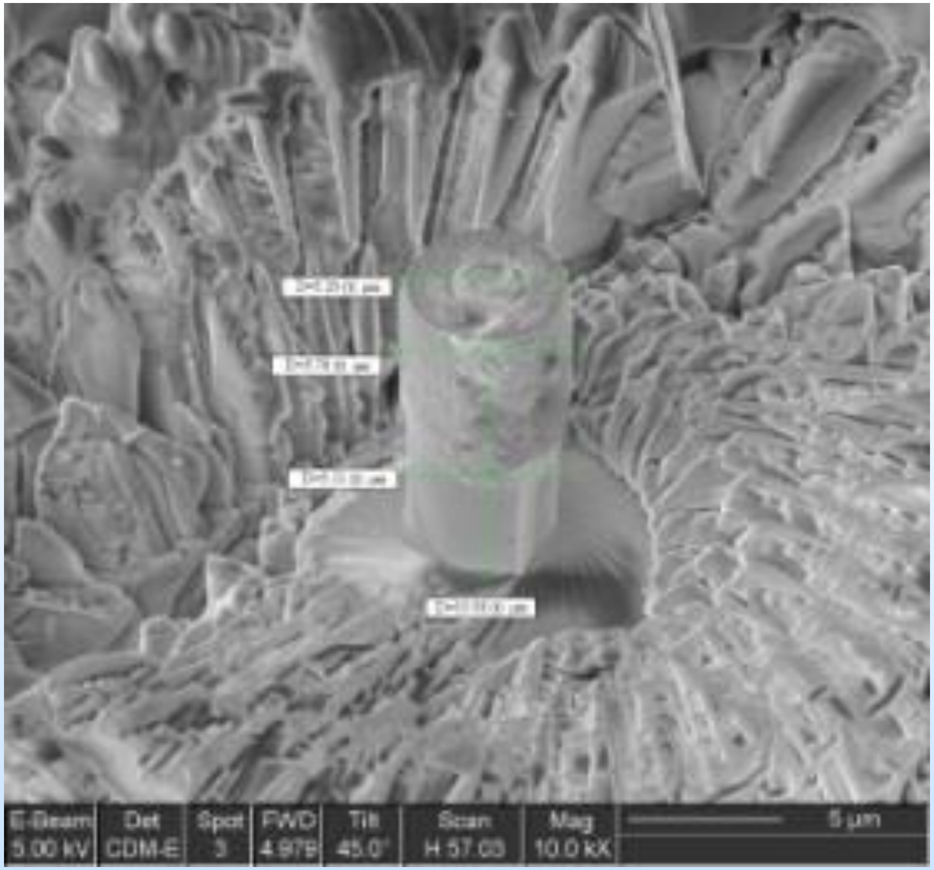


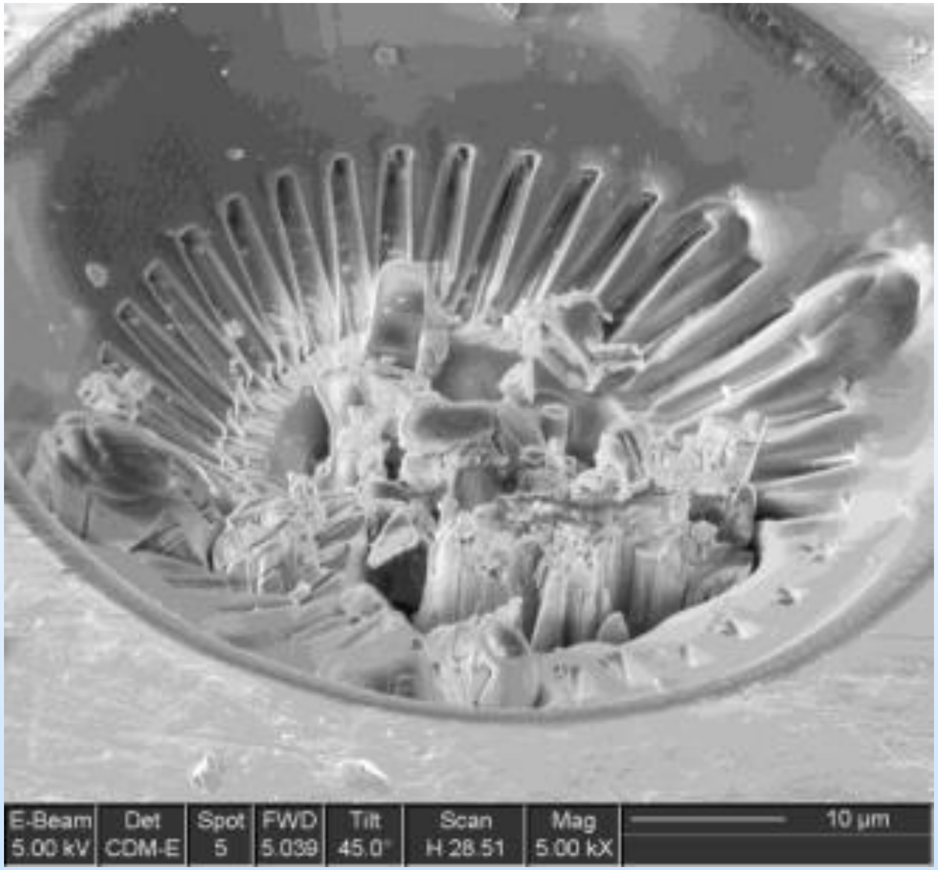


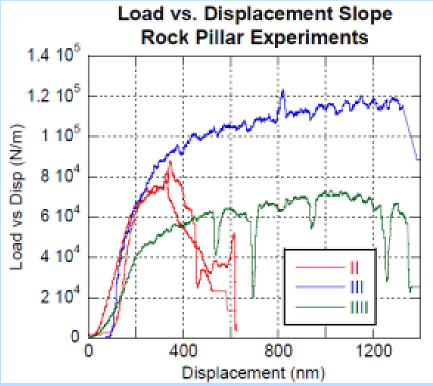


- Focused Ga+ Ion Milling and SEM imaging , including pillar machining and slice-and-view
- Micropillar compression (load vs. displacement) performed with a nanoindenter and flat diamond indenter

# Conclusions

- Macroscopic and microscopic lithofacies have distinctively different mechanical properties.
- Bulk properties may be misleading as they can represent averages of mechanically heterogeneous rock.
- Microscopic heterogeneity controls the spatial distribution of fractures.
- Micro fractures may link up through failure of micro-relays to form through-going fractures.
- Mode of strain distribution is in some respects scale independent.

# Acknowledgements

This work was funded by the U.S. Department of Energy, Office of Science, Basic Energy Sciences under Award Number DE-SC0006883.

Sandia National Laboratories is a multi-program laboratory managed and operated by Sandia Corporation, a wholly owned subsidiary of Lockheed Martin Corporation, for the U.S. Department of Energy's National Nuclear Security Administration under contract DE-AC04-94AL85000.

A few reference slides

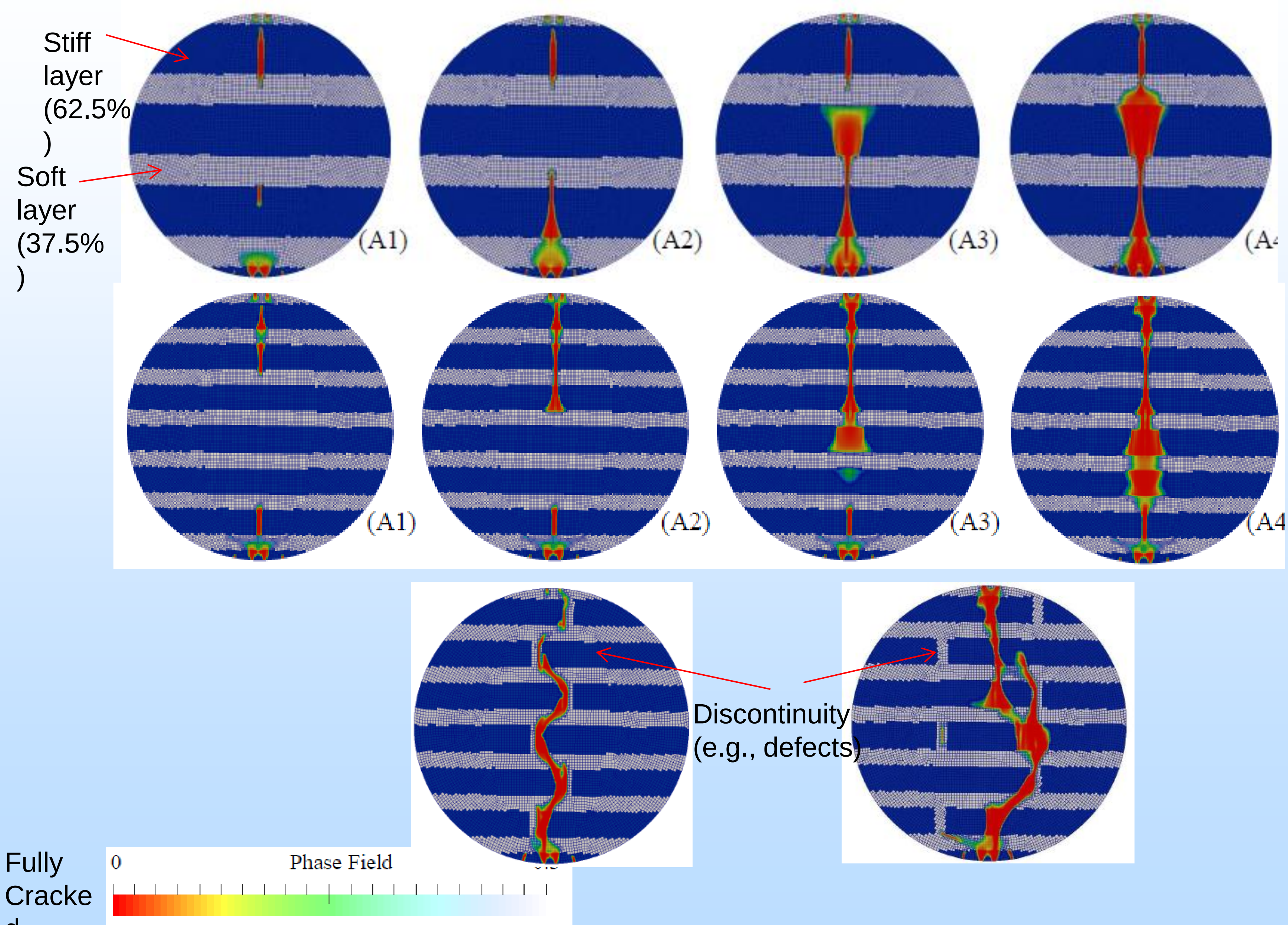
Stiff layer (62.5%)
Soft layer (37.5%)
(A1)
(A2)
(A3)
(A4
(A1)
(A2)
(A3)
(A4
Discontinuity (e.g., defects)
Fully Cracked
0
Phase Field

# Multiscale characterization of physical, chemical, and mechanical heterogeneity of shale

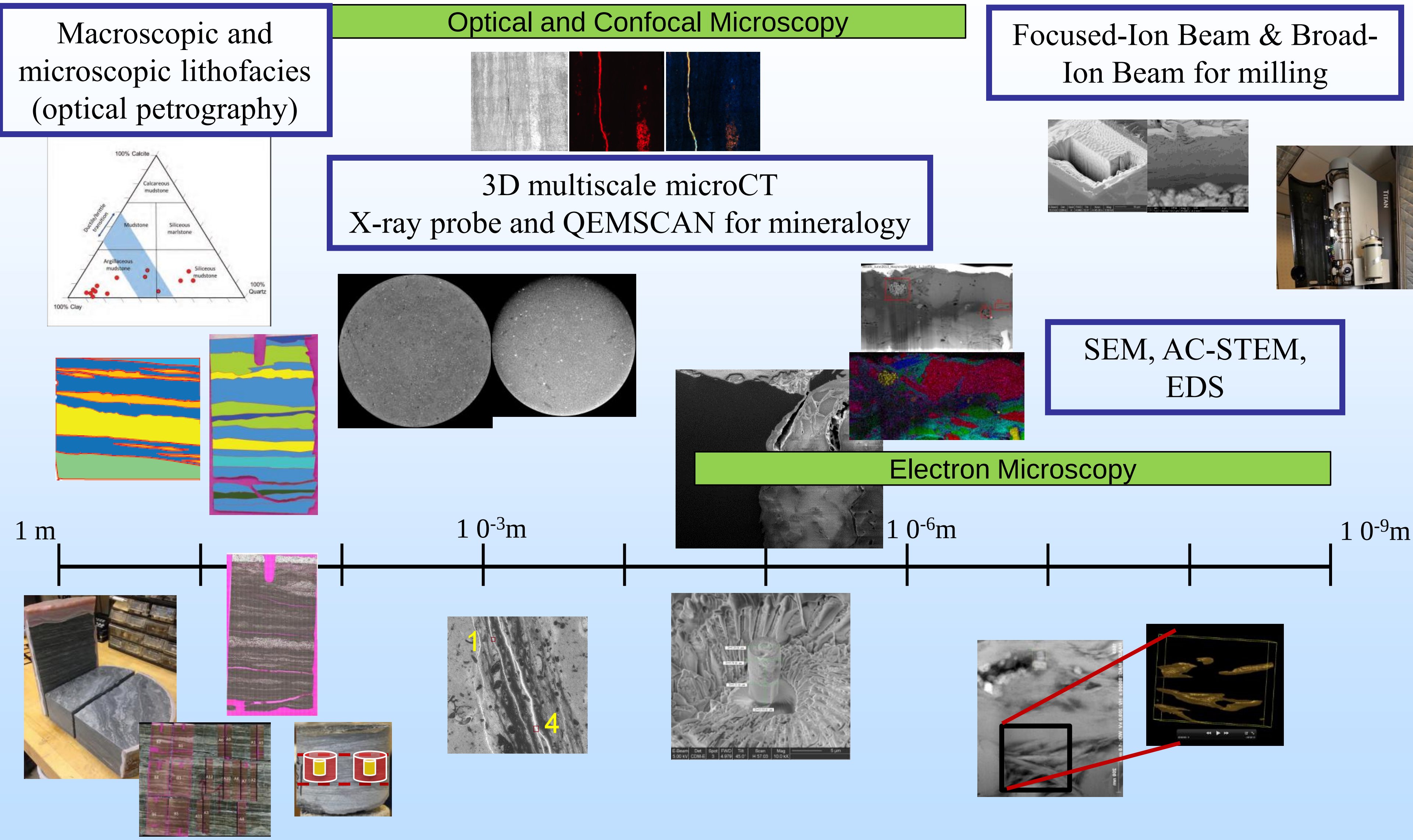

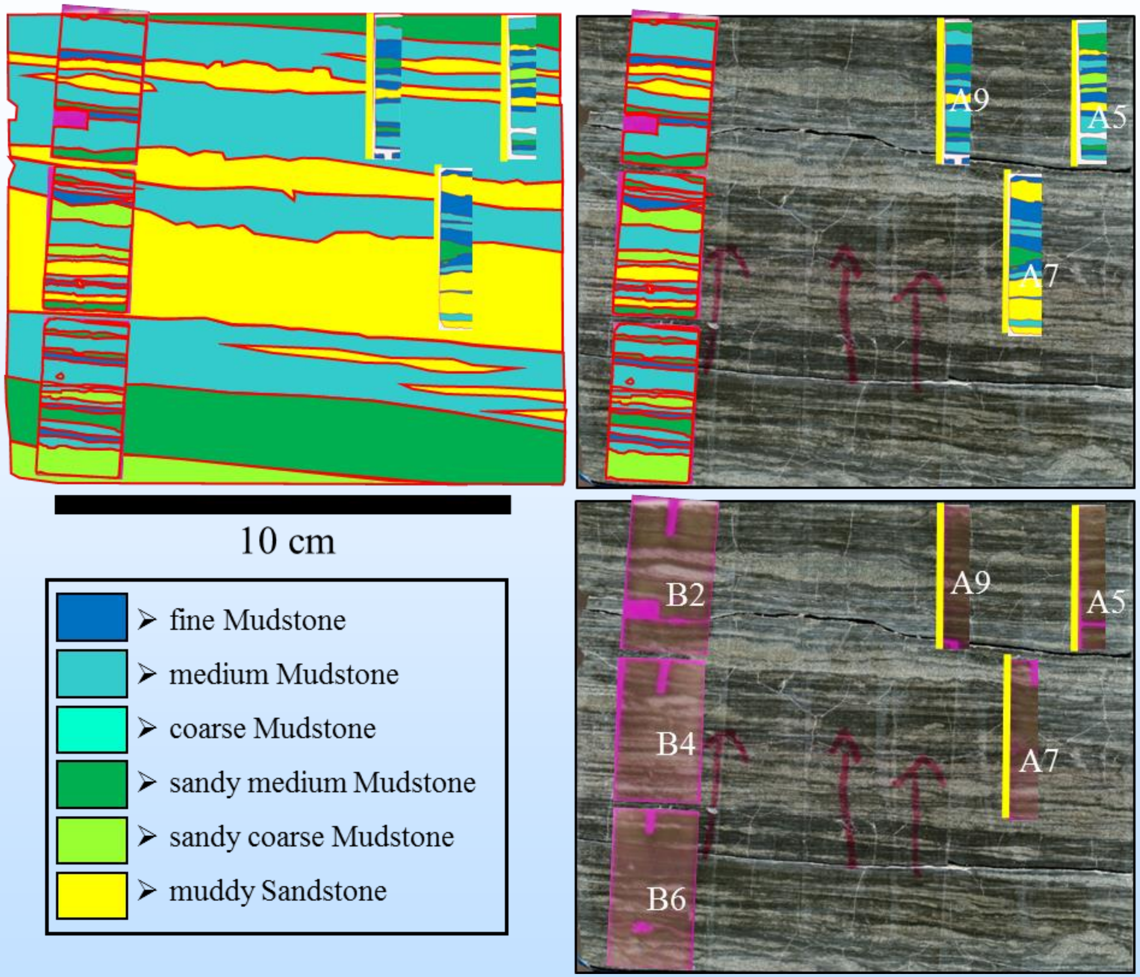
A9
A5
A7
10 cm
fine Mudstone
medium Mudstone
coarse Mudstone
sandy medium Mudstone
sandy coarse Mudstone
muddy Sandstone
B2
A9
A5
B4
A7
B6

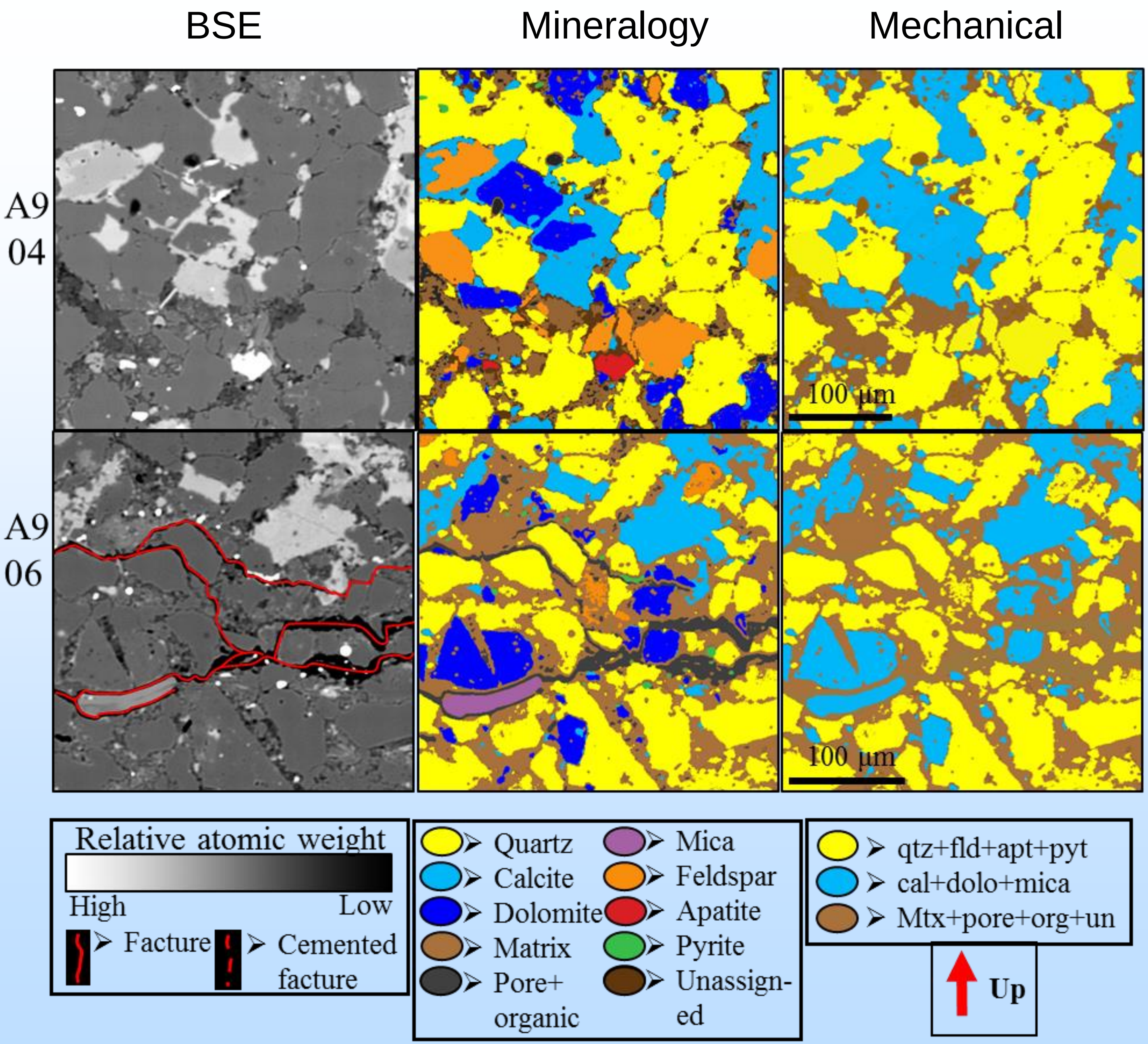
BSE
Mineralogy
Mechanical
A9 04
A9 06
100 µm
100 µm
Relative atomic weight
High
Low
Facture
Cemented facture
Quartz
Calcite
Dolomite
Matrix
Pore+ organic
Mica
Feldspar
Apatite
Pyrite
Unassign-ed
qtz+fld+apt+pyt
cal+dolo+mica
Mtx+pore+org+un
Up

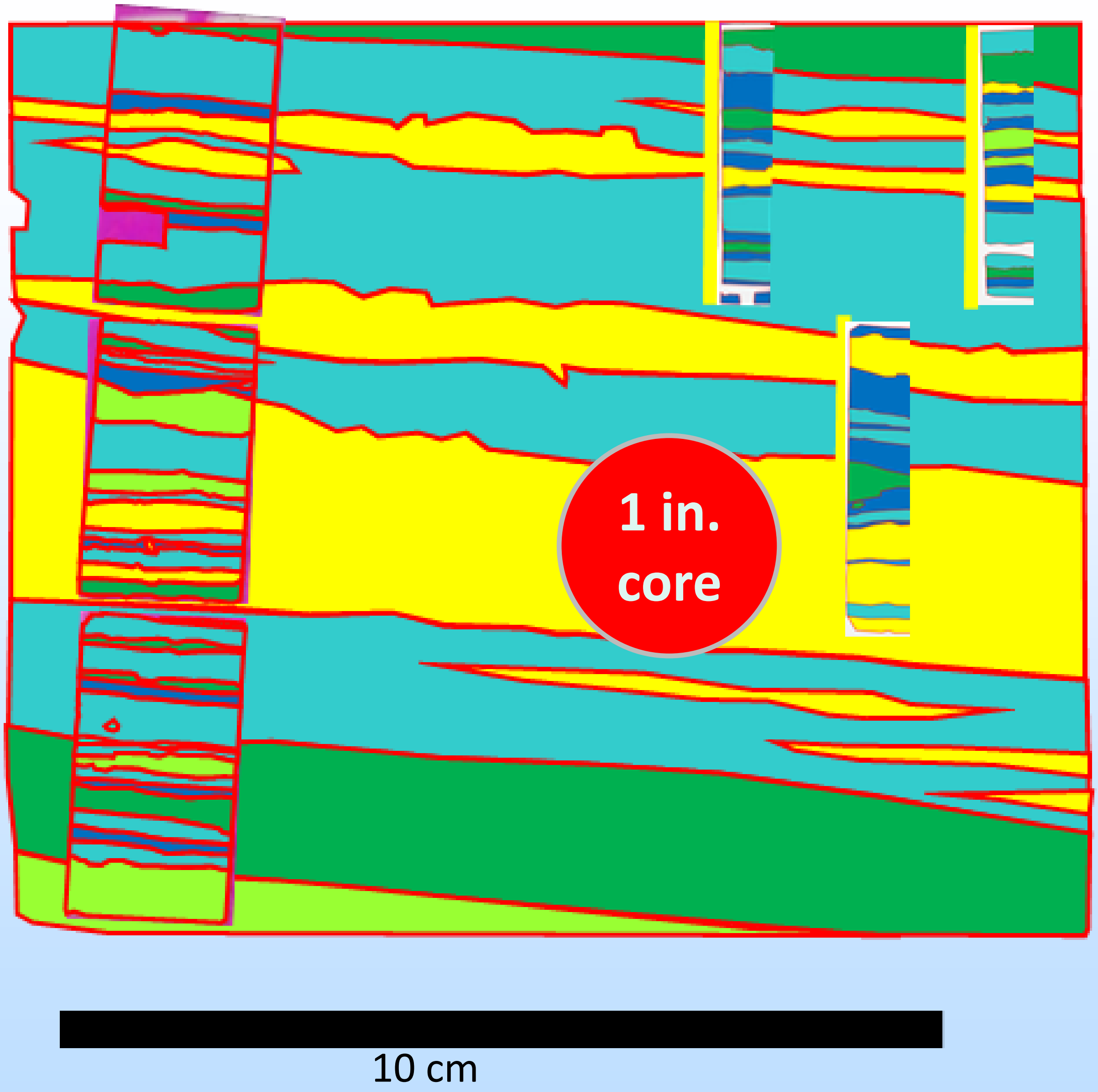
1 in.
core
10 cm

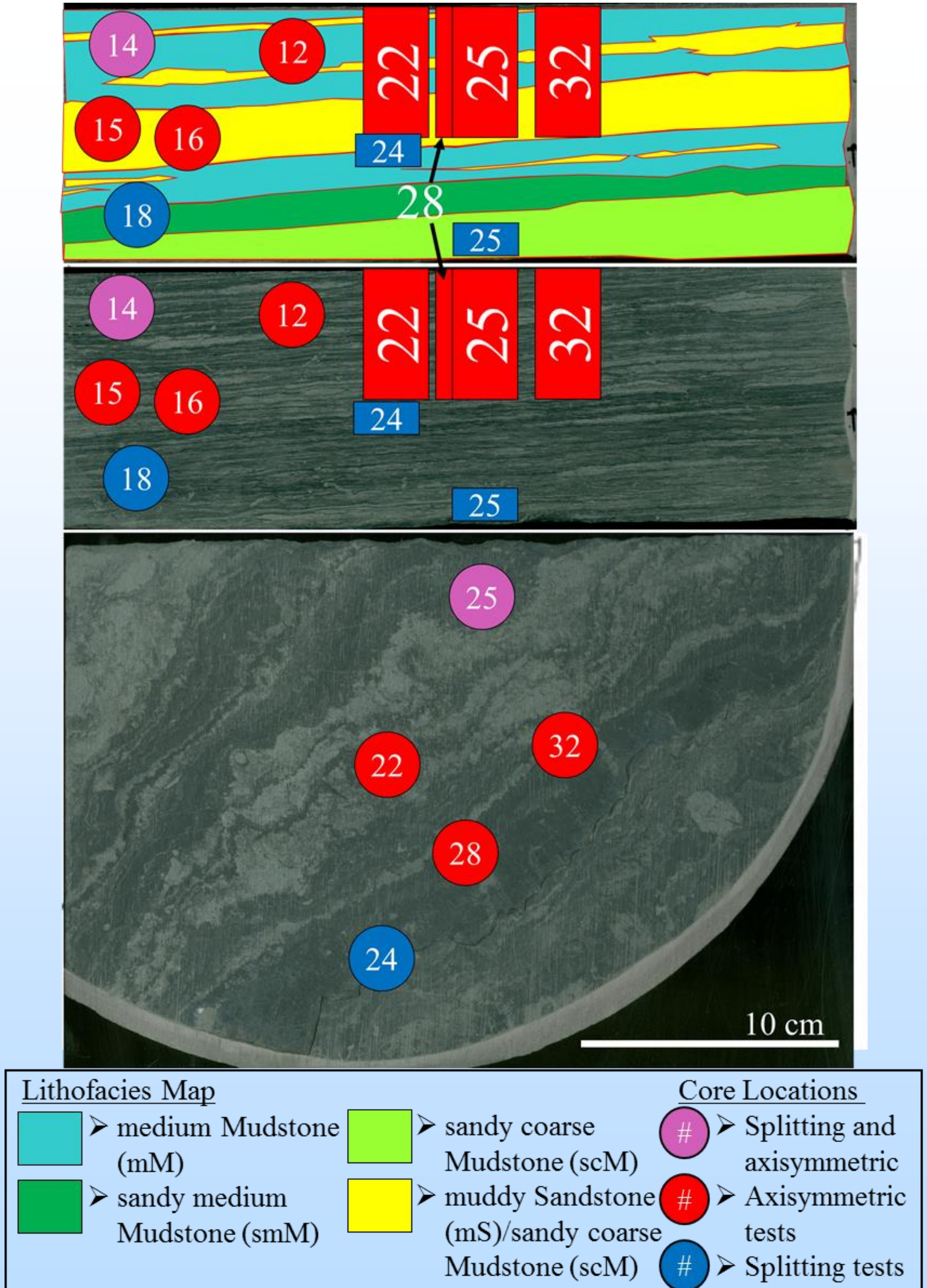
14
12
22
25
32
15
16
24
28
18
25
10 cm
Lithofacies Map
➢ medium Mudstone (mM)
➢ sandy medium Mudstone (smM)
➢ sandy coarse Mudstone (scM)
➢ muddy Sandstone (mS)/sandy coarse Mudstone (scM)
Core Locations
# ➢ Splitting and axisymmetric
# ➢ Axisymmetric tests
# ➢ Splitting tests

# Sample Orientation

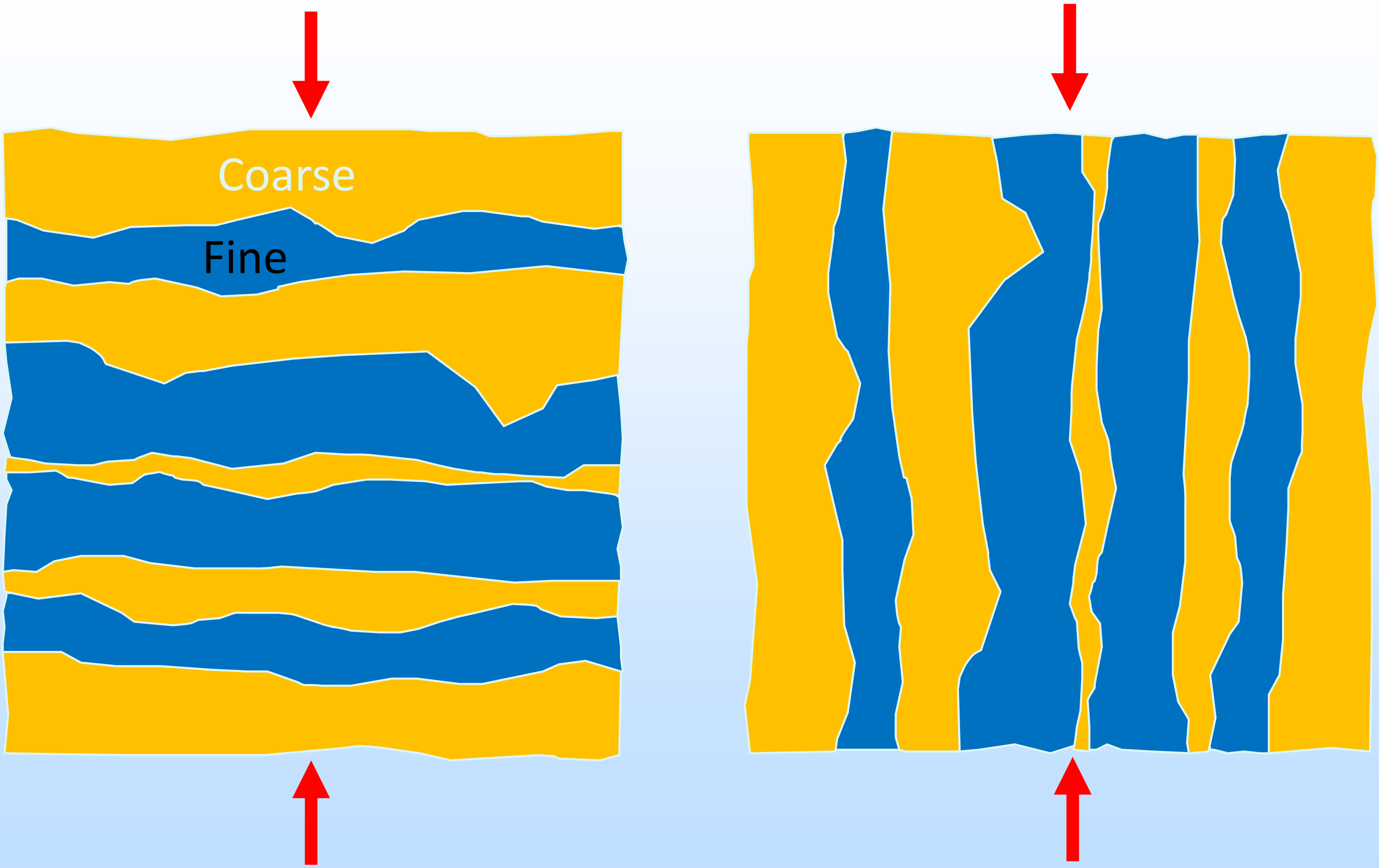

Experimental Determination of failure and response of Mancos shale parallel and perpendicular to the bedding plane.

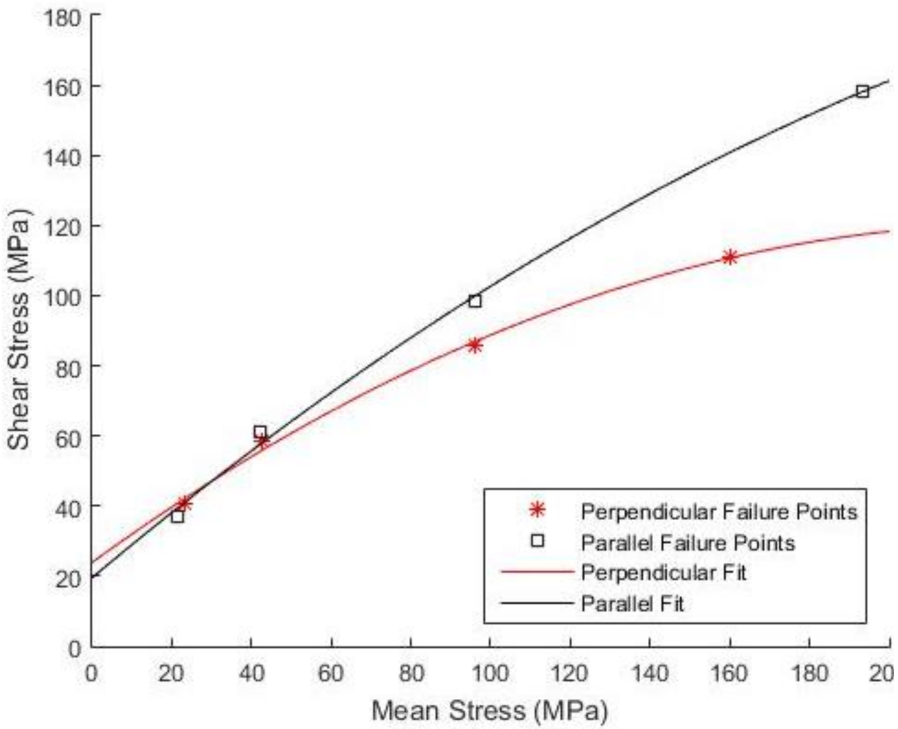


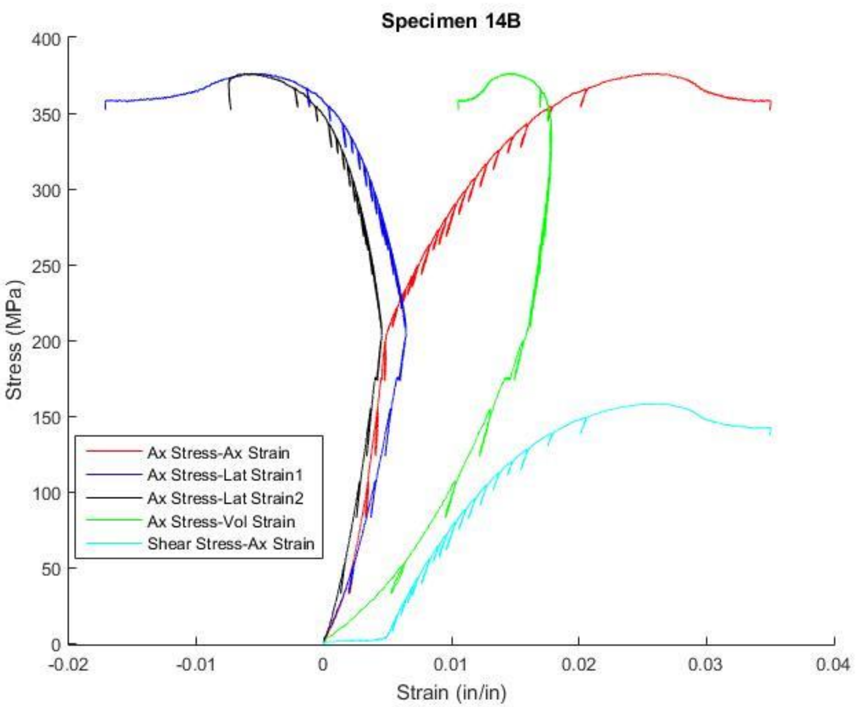


Above Left: difference between failure parallel and perpendicular to bedding, perpendicular to bedding shows a large drop in strength as mean stress increases compared with parallel to bedding.
Above Right: Example stress–strain plots for a test
Far Left: Specimen cored perpendicular to bedding, tested unconfined
Near Left: Specimen (14B) cored parallel to bedding, tested at 200 MPa constant mean stress, this is the sample shown in the plot above right.

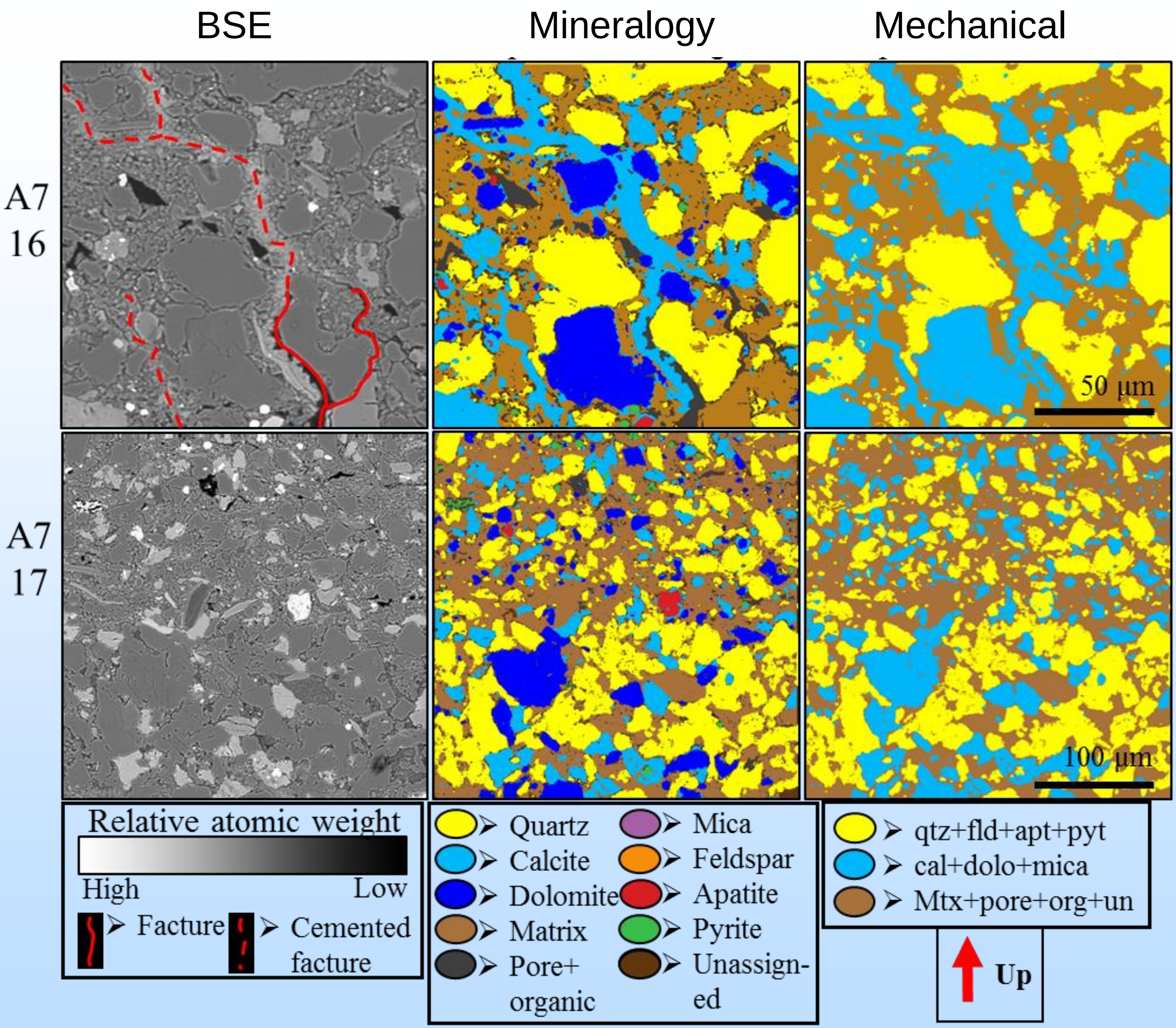
BSE
Mineralogy
Mechanical
A7 16
A7 17
50 µm
100 µm
Relative atomic weight
High
Low
Facture
Cemented facture
Quartz
Calcite
Dolomite
Matrix
Pore+ organic
Mica
Feldspar
Apatite
Pyrite
Unassign- ed
qtz+fld+apt+pyt
cal+dolo+mica
Mtx+pore+org+un
Up

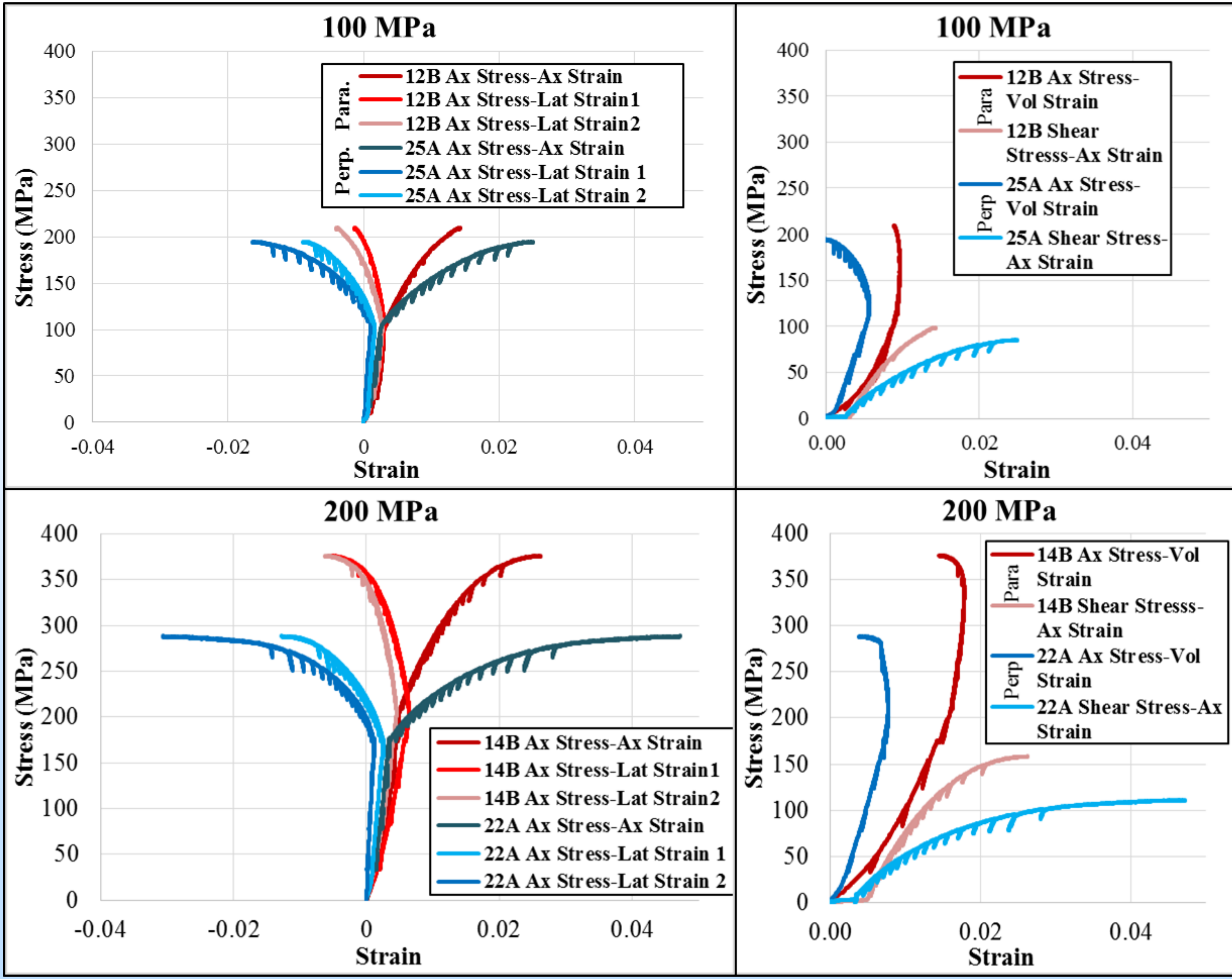
100 MPa
Stress (MPa)
Strain
Para.
Perp.
12B Ax Stress-Ax Strain
12B Ax Stress-Lat Strain1
12B Ax Stress-Lat Strain2
25A Ax Stress-Ax Strain
25A Ax Stress-Lat Strain 1
25A Ax Stress-Lat Strain 2
100 MPa
Stress (MPa)
Strain
Para
Perp
12B Ax Stress-Vol Strain
12B Shear Stresss-Ax Strain
25A Ax Stress-Vol Strain
25A Shear Stress-Ax Strain
200 MPa
Stress (MPa)
Strain
14B Ax Stress-Ax Strain
14B Ax Stress-Lat Strain1
14B Ax Stress-Lat Strain2
22A Ax Stress-Ax Strain
22A Ax Stress-Lat Strain 1
22A Ax Stress-Lat Strain 2
200 MPa
Stress (MPa)
Strain
Para
Perp
14B Ax Stress-Vol Strain
14B Shear Stresss-Ax Strain
22A Ax Stress-Vol Strain
22A Shear Stress-Ax Strain

# Shale Poromechanics:
# Heterogeneity, Flow, Failure, and Creep

## Mechanical testing of failure

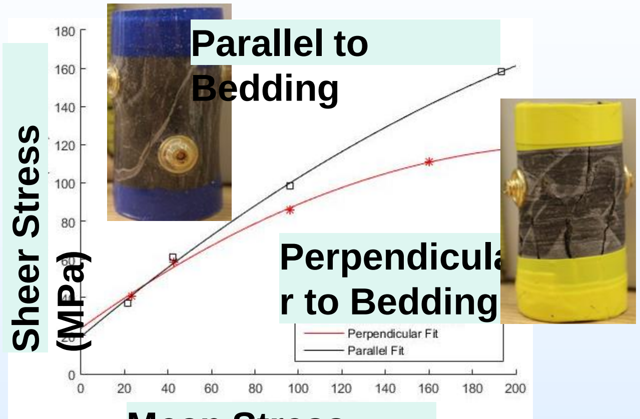


A large drop in strength as mean stress increases for perpendicular to bedding

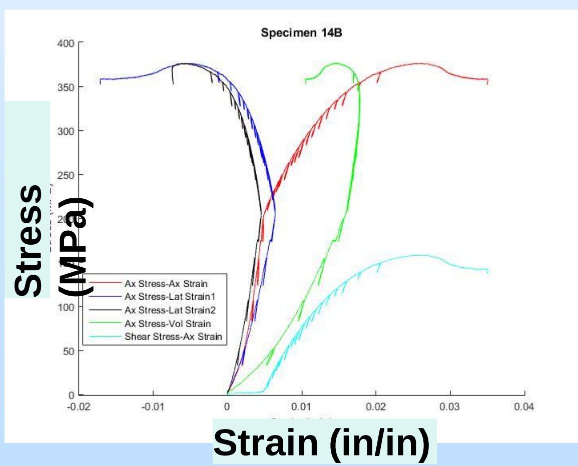


Example stress–strain plots for a test: Specimen (14B) cored parallel to bedding, tested at 200 MPa constant mean stress

## Micropillar Compression Testing

- Focused Ga+ Ion Milling and SEM imaging , including pillar machining and slice-and-view
- Micropillar compression (load vs. displacement) performed with a nanoindenter and flat diamond indenter

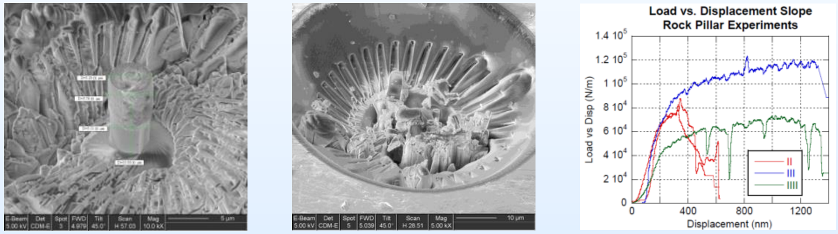


## Pulse Decan Experiment for Permeability and Porosity

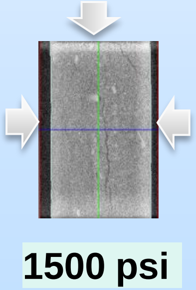


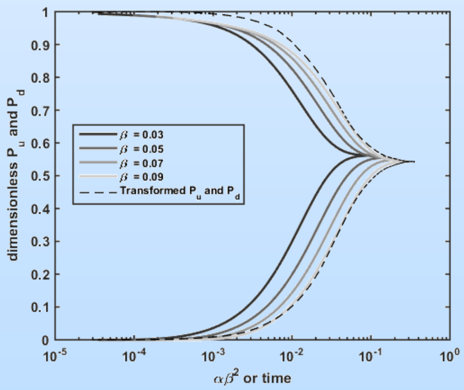


Mathematical development and validation for estimating permeability and porosity of tight rocks using type curve matching and Pseudo pressure

# MicroCT Imaging of shale

- Multiple scale micro-CT image stacks for Mancos shale and Marcellus shale are used to characterize the impact of heterogeneous materials (fractures and laminated materials) on mechanical properties of shale

MicroCT image of 1” core Mancos shale (17 microns resolution)

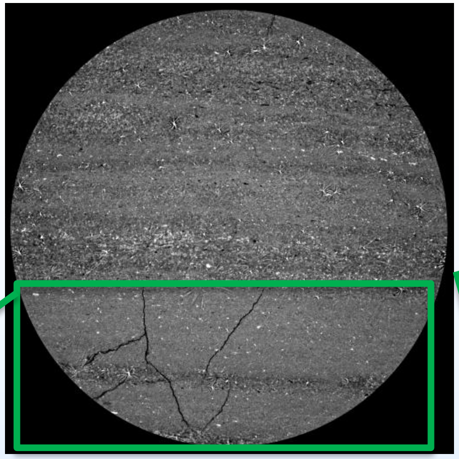

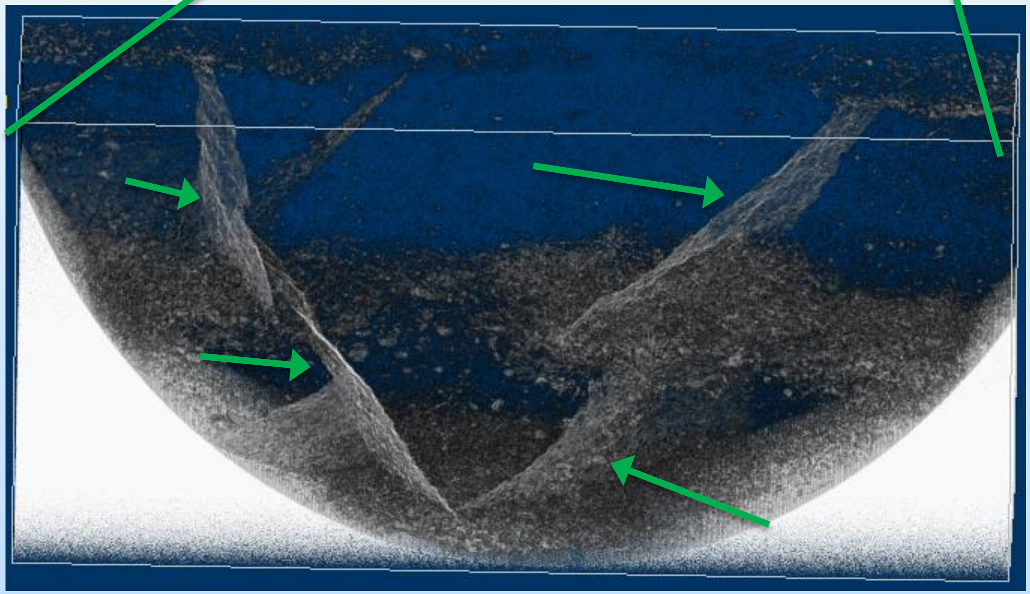

3D view of natural and artificial fractures (arrows) in clay-rich weak layers terminated by stiff layers. Relatively large white spots represent pyrites that are used to estimate 3D deformation of shale during mechanical testing